"Workshop on Ocean Wave Dynamics"
Toronto, Ontario, May 6-11, 2013

Rogue Waves – higher order structures

N. Akhmediev

The Australian National University, Canberra, ACT 0200, Australia

Abstract

Peregrine breather being the lowest order rational solution of the nonlinear Schrodinger equation is commonly considered as a prototype of a rogue wave in the ocean. Higher-order rational solutions are far from being as simple as the Peregrine breather itself. They are not as simple as a nonlinear superposition of solitons either. Only recently, the complexity of their spatio-temporal structures started to be revealed. Basic thoughts on their classification will be presented in this talk.

Rogue wave in a laboratory, Hamburg

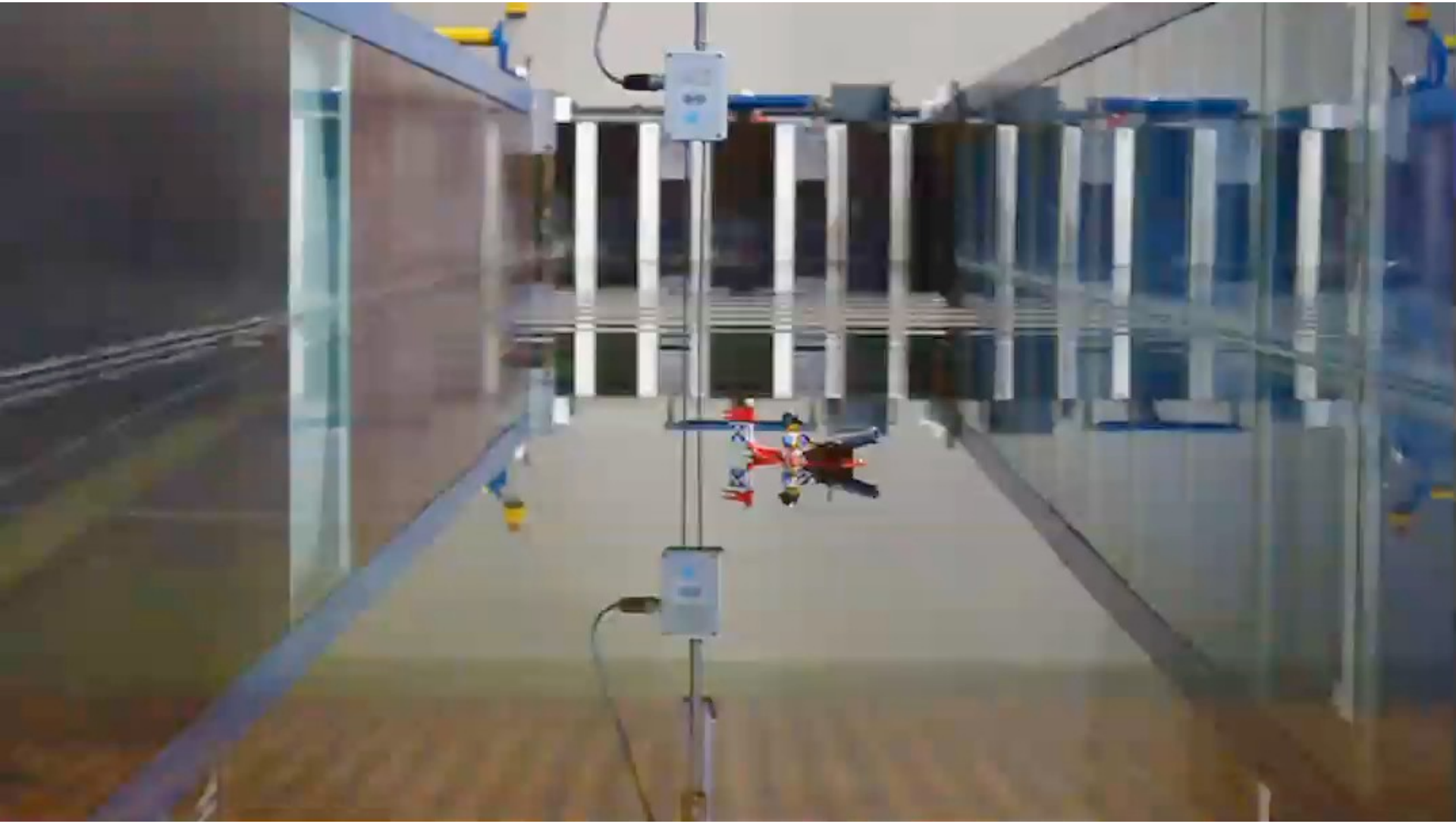

Amin Chabchoub et al, Phys. Rev. X 2, 011015 (2012)

Rogue wave in the sea

Rogue waves in the ocean

A print by Katsushika Hokusai (1760-1849) ‘Fast Cargo Boat Battling the Waves’

In 1978, the München, a German barge carrier, sank in the Atlantic.

What kind of a wave is Hokusai’s “Great wave off Kanagawa”

By J. Cartwright and H. Nakamura

Recorded rogue waves

The Draupner platform is a key hub for monitoring pressure, volume and quality of gas flows in the Norway's offshore gas pipelines.

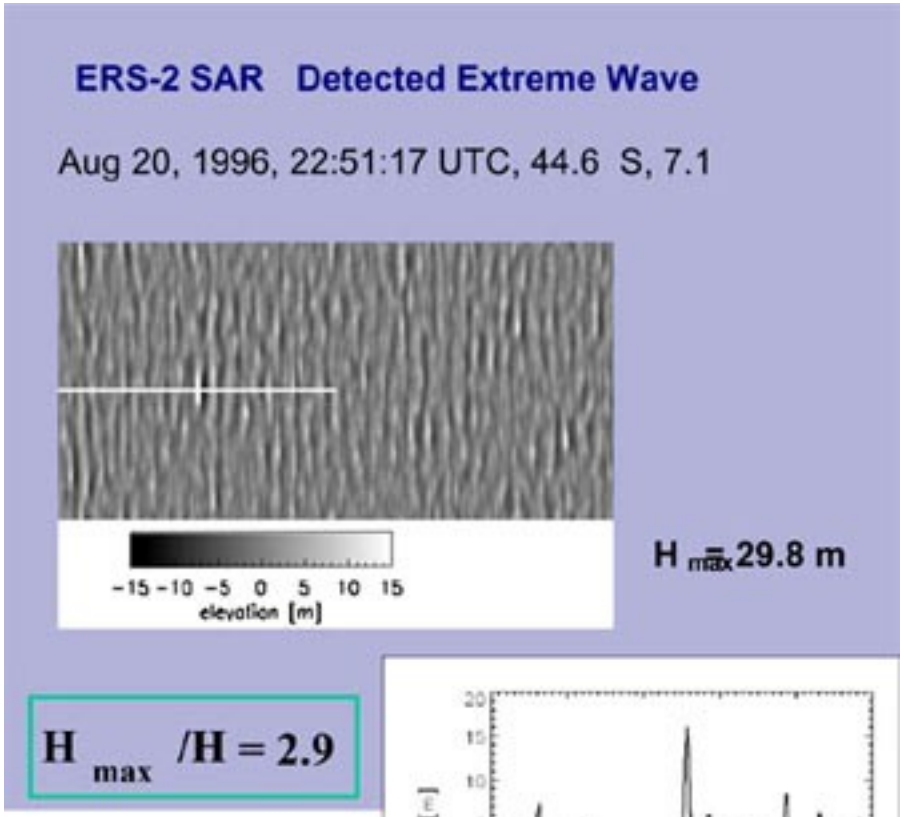

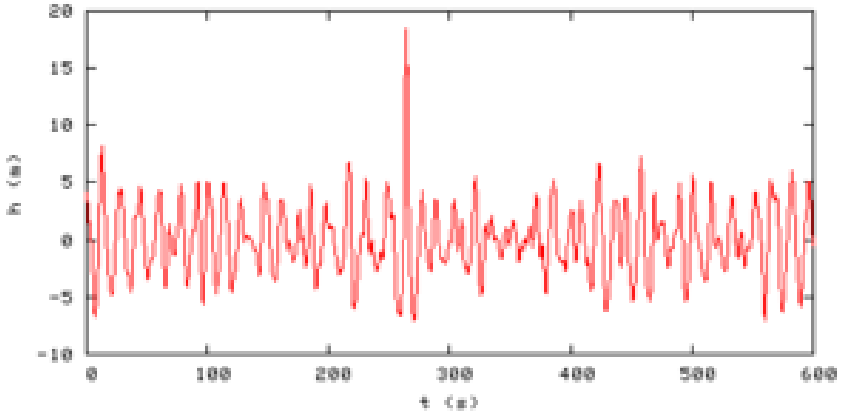

The Draupner wave, a single giant wave measured on New Year's Day 1995, finally confirmed the existence of freak waves, which had previously been considered near-mythical

Optical Rogue Waves

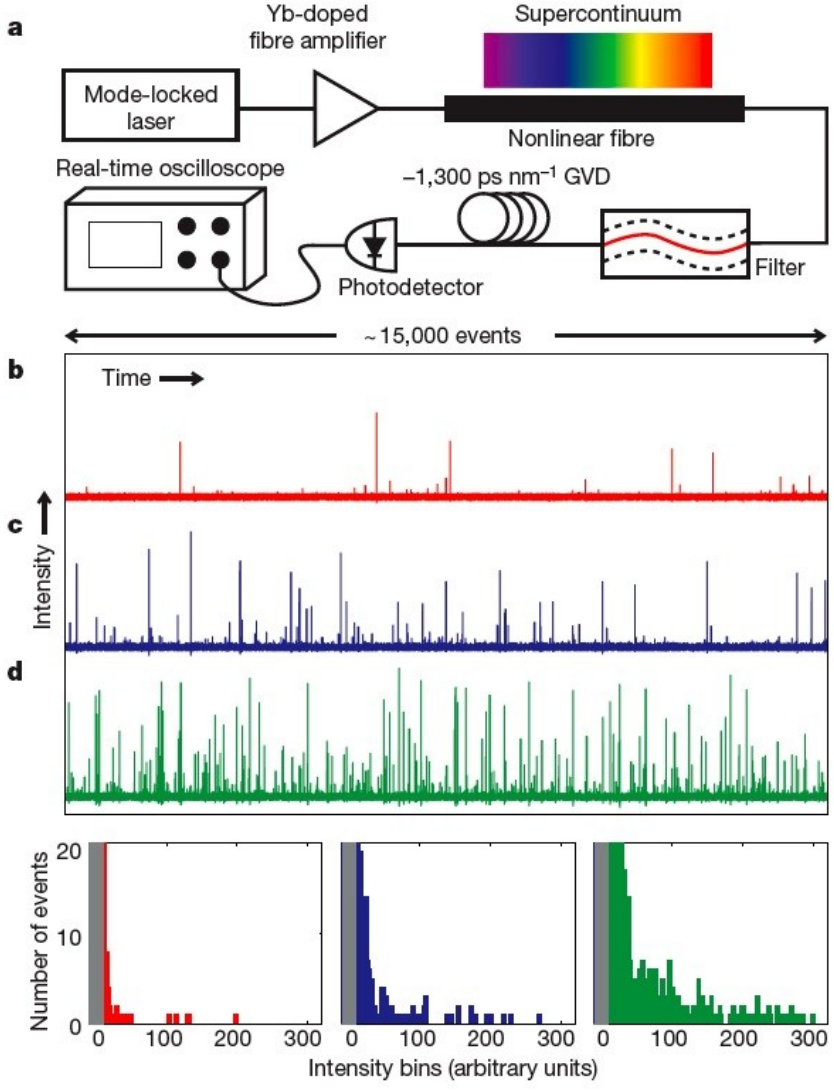

NATURE|Vol 450|13 December 2007

Optical rogue waves

D. R. Solli[1], C. Ropers[1,2], P. Koonath[1] & B. Jalali[1]

Figure 1 | Experimental observation of optical rogue waves. **a**, Schematic of experimental apparatus. **b–d**, Single-shot time traces containing roughly 15,000 pulses each and associated histograms (bottom of figure: left, **b**; middle, **c**; right, **d**) for average power levels 0.8 μW (red), 3.2 μW (blue) and 12.8 μW (green), respectively. The grey shaded area in each histogram demarcates the noise floor of the measurement process. In each measurement, the vast majority of events (>99.5% for the lowest power) are buried in this low intensity range, and the rogue events reach intensities of at least 30–40 times the average value. These distributions are very different from those encountered in most stochastic processes.

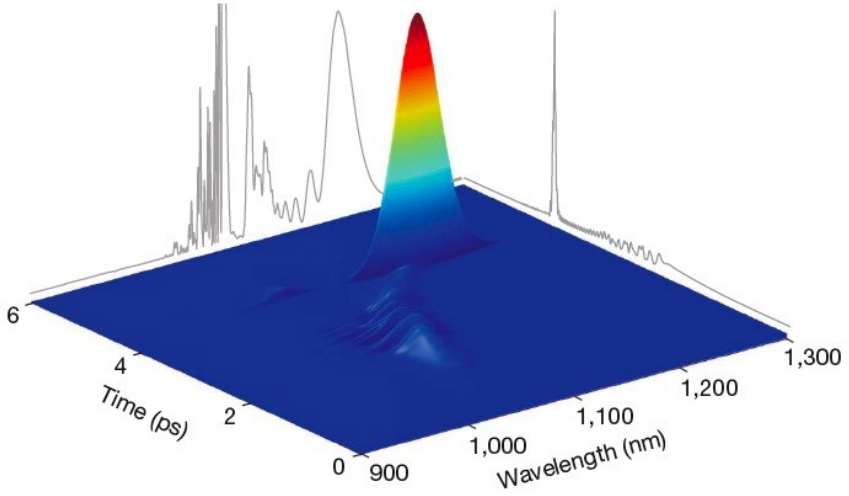

Figure 3 | Time–wavelength profile of an optical rogue wave obtained from a short-time Fourier transform. The optical wave has broad bandwidth and

Rogue waves are ubiquitous

PRL 103, 173901 (2009) PHYSICAL REVIEW LETTERS week ending 23 OCTOBER 2009

Non-Gaussian Statistics and Extreme Waves in a Nonlinear Optical Cavity

A. Montina,[1] U. Bortolozzo,[2] S. Residori,[2] and F. T. Arecchi[1,3]

[1]*Dipartimento di Fisica, Università di Firenze, via Sansone 1, 50019 Sesto Fiorentino (FI), Italy*
[2]*INLN, Université de Nice Sophia-Antipolis, CNRS, 1361 route des Lucioles 06560 Valbonne, France*
[3]*INOA-CNR, largo E. Fermi 6, 50125 Firenze, Italy*

(Received 19 February 2009; published 19 October 2009)

M. S. Ruderman,

University of Sheffield,

Freak waves in laboratory and

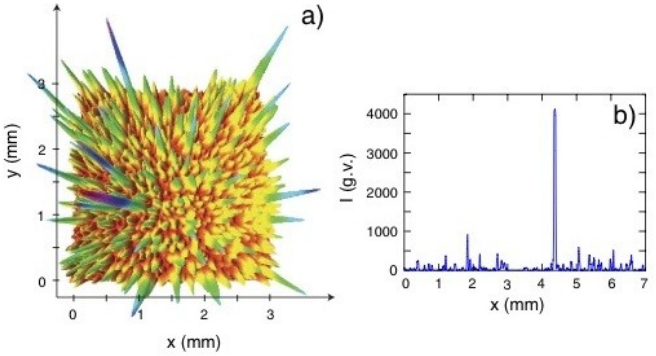

FIG. 1 (color online). (a) Instantaneous experimental profile of the transverse intensity distribution; (b) a 1D profile showing an extreme event; I is measured in gray values, g.v.

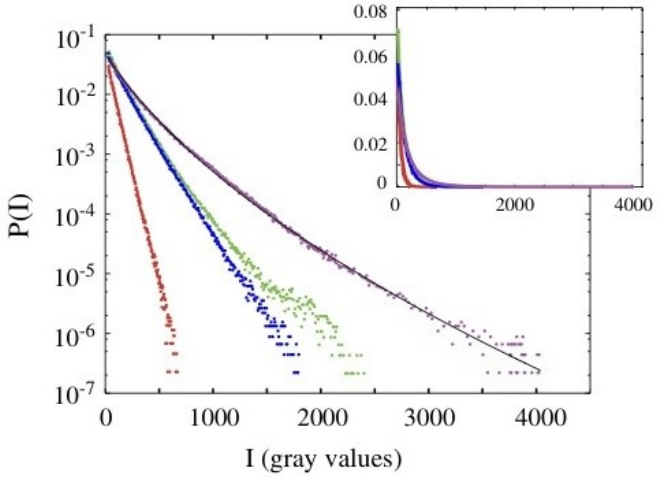

FIG. 2 (color online). Experimental PDF of the cavity field

J. Plasma Physics (2010), *vol.* 76, *parts* 3&4, *pp.* 293–295. © Cambridge University Press 2010
doi:10.1017/S0022377809990481

Rogue waves in the atmosphere

LENNART STENFLO[1] and MATTIAS MARKLUND[2]

[1]Department of Physics, Linköping University, SE-581 83 Linköping, Sweden
[2]Department of Physics, Umeå University, SE-901 87 Umeå, Sweden
(mattias.marklund@physics.umu.se)

Rogue waves in superfluid helium

V. B. Efimov[1,2,a], A. N. Ganshin[1,b], G. V. Kolmakov[1,3,c], P. V. E. McClintock[1,d], and L. P. Mezhov-Deglin[2,e]

[1] Department of Physics, Lancaster University, Lancaster, LA1 4YB, UK
[2] Institute of Solid State Physics RAS, Chernogolovka, Moscow region, 142432, Russia
[3] Department of Chemical and Petroleum Engineering, Pittsburgh University, Pittsburgh, PA 15261, USA.

Rogue waves in finances

The Pricing of Options and Corporate Liabilities

Fischer Black

University of Chicago

Myron Scholes

Massachusetts Institute of Technology

Journal of Political Economy, 81, 637 (1973)

Merton and Scholes received the 1997 Nobel Prize in

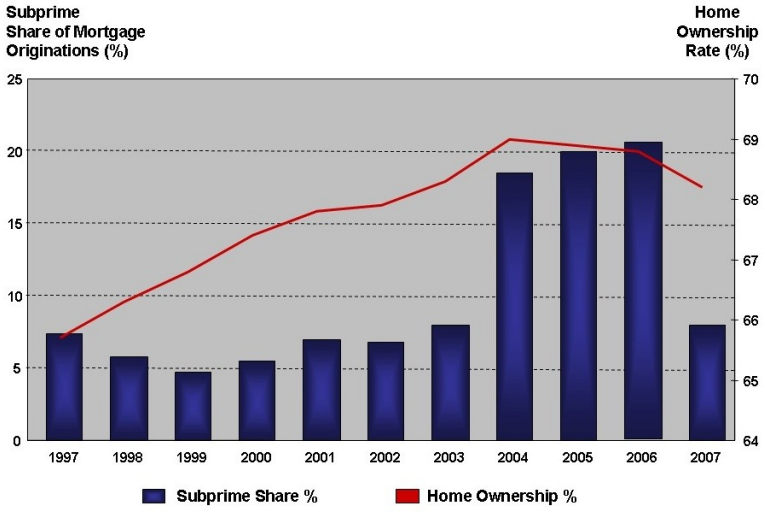

Sources: U.S. Census Bureau; Harvard University- State of the Nation's Housing Report 2008

US Subprime lending expanded significantly in the years

2004-2006 preceding the economic crisis

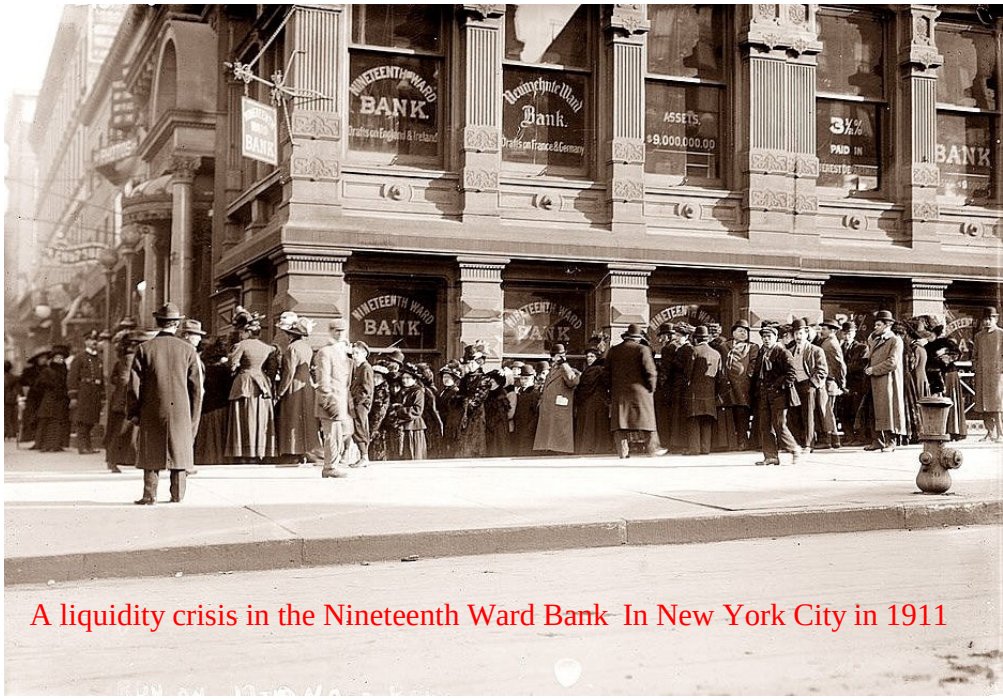

A liquidity crisis in the Nineteenth Ward Bank In New York City in 1911

New Financial Research Program:
General Option-Price Wave Modeling

Vladimir G. Ivancevic

Defence Science & Technology Organisation, Australia

Financial rogue waves

Zhenya Yan[a,b]

[a] *Centro de Física Teórica e Computacional, Universidade de Lisboa, Complexo Interdisciplinar, Lisboa 1649-003, Portugal*

[b] *Key Laboratory of Mathematics Mechanization, Institute of Systems Science, AMSS, Chinese Academy of Sciences, Beijing 100190, China*

Two forms of the NLS equation

$$i\left(\frac{\partial \psi}{\partial t} + C_{gr}\frac{\partial \psi}{\partial x}\right) + \frac{\sqrt{gk_0}}{8k_0^2}\frac{\partial^2 \psi}{\partial x^2} + \frac{\sqrt{gk_0}}{2}k_0^2|\psi|^2\psi = 0$$

Water surface elevation:

$$\eta = \mathrm{Re}[\psi(x,t)\exp(i\omega_0 t - ik_0 x)]$$

Dispersion relation:

$$\omega_0^2 = gk_0$$

Group velocity:

$$C_{gr} = \frac{\omega_0}{2k_0}$$

$$i\left(\frac{\partial \psi}{\partial x} + \frac{1}{C_{gr}}\frac{\partial \psi}{\partial t}\right) + \frac{1}{g}\frac{\partial^2 \psi}{\partial t^2} + \frac{\omega_0^6}{g^3}|\psi|^2\psi = 0$$

A. Osborne, Nonlinear ocean waves and the inverse scattering transform (Academic Press, 2010)

K. Trulsen, Weakly nonlinear and stochastic properties of ocean wave fields: application to an extreme wave event. In: Waves in geophysical fluids: Tsunamis, Rogue waves, Internal waves and Internal tides. Eds.: Grue, J. \& Trulsen, K. CISM Courses and Lectures No. 489, (Springer, NY, Wein, 2006).

Modulation instability and FPU

$$i\frac{\partial y}{\partial x}+\frac{1}{2}\frac{\partial^2 y}{\partial t^2}+|y|^2 y=0$$

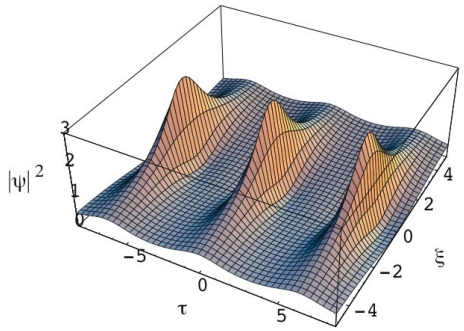

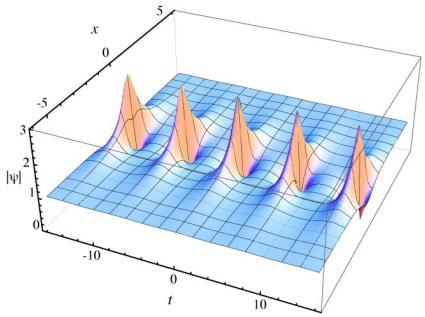

Benjamin-Fair (Bespalov-Talanov) instability:

$$\psi\approx\left[1+\left(a\left(1+i\frac{2d}{k^2}\right)e^{dx}+b\left(1-i\frac{2d}{k^2}\right)e^{-dx}\right)\cos kt\right]\exp(ix)$$

The simplest form of Akhmediev breather:

$$\psi=\frac{\cos(\sqrt{2}t)+i\sqrt{2}\sinh x}{\cos(\sqrt{2}t)-i\sqrt{2}\sinh x}\exp(ix)$$

Growth rate of instability:

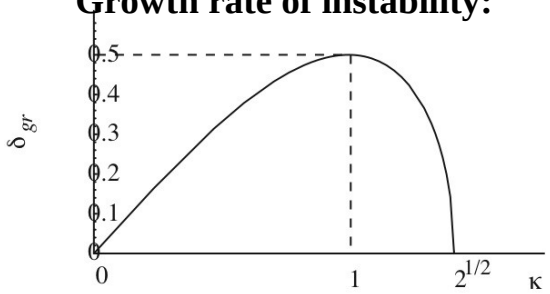

$$\delta=k\sqrt{1-\frac{k^2}{4}}$$

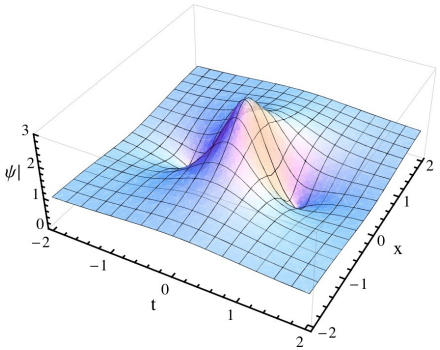

MODULATION INSTABILITY AND PERIODIC SOLUTIONS OF THE NONLINEAR SCHRÖDINGER EQUATION

N. N. Akhmediev and V. I. Korneev

Translated from Teoreticheskaya i Matematicheskaya Fizika, Vol. 69, No. 2, pp. 189-194, November, 1986. Original article submitted July 23, 1985.

0040-5779/86/6902-1089$12.50

Modulation instability, ABs and continuous wave supercontinuum generation

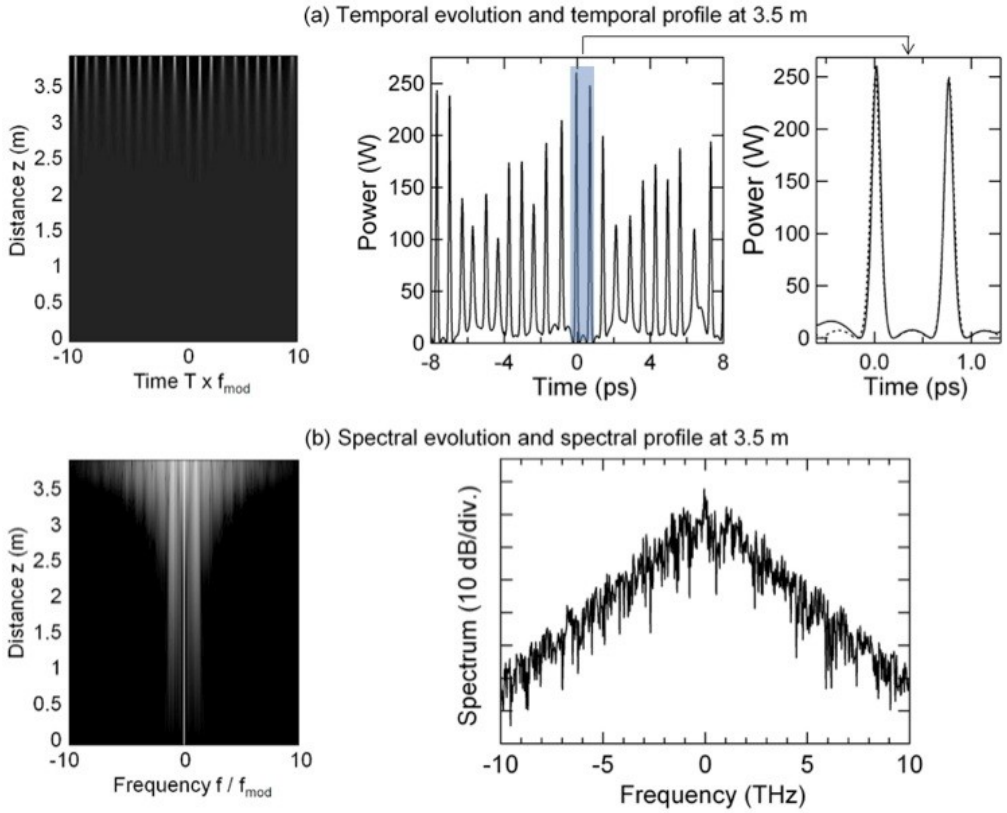

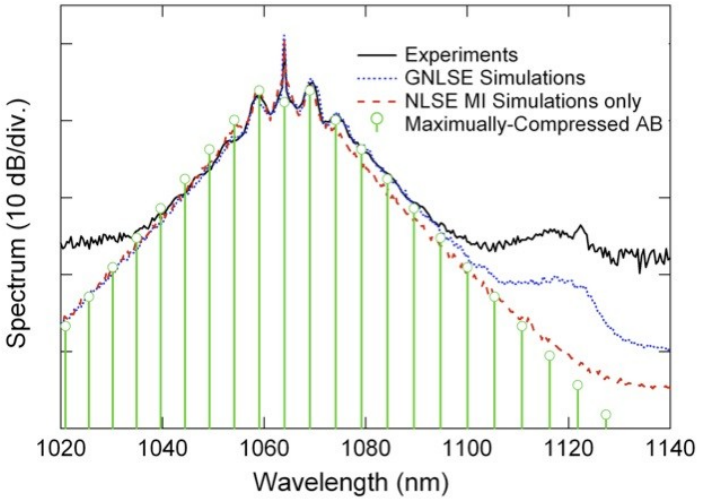

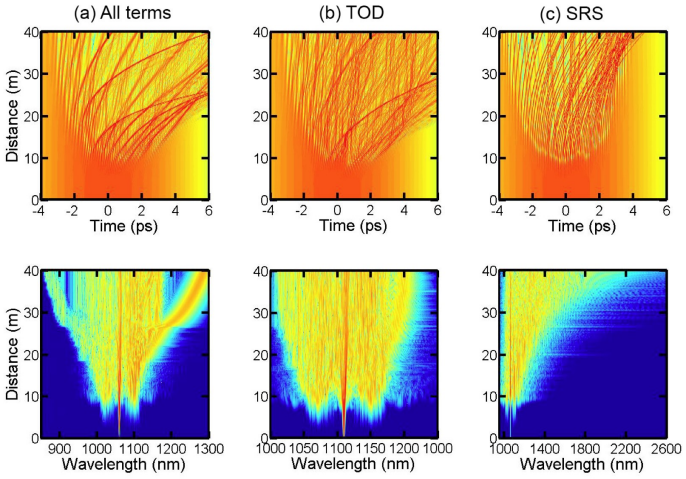

Dudley et al., Optics Express, 17, No 24, 21497 (2009)

NLSE and variety of its solutions

$$i\frac{\partial y}{\partial x}+\frac{1}{2}\frac{\partial^2 y}{\partial t^2}+|y|^2 y=0$$

Rational soliton

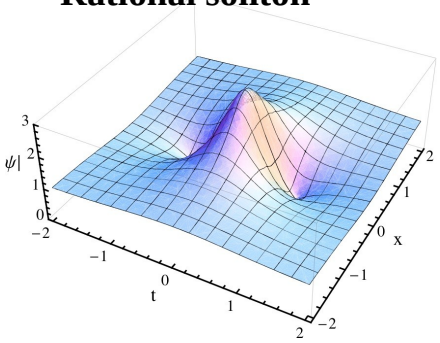

Double periodic solution

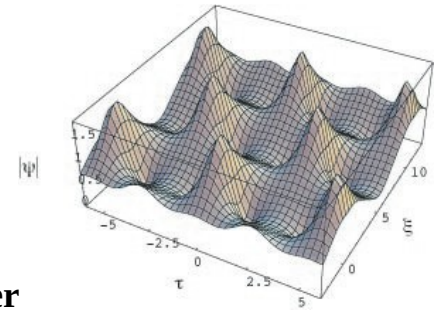

Kuznetsov-Ma soliton

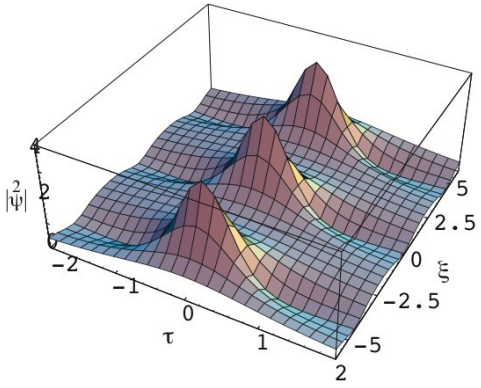

Akhmediev breather

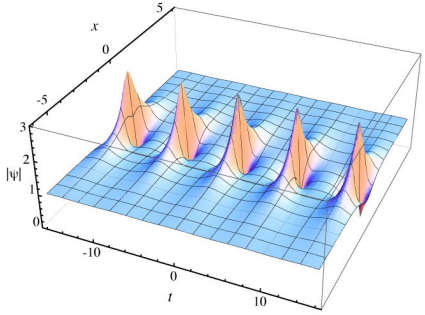

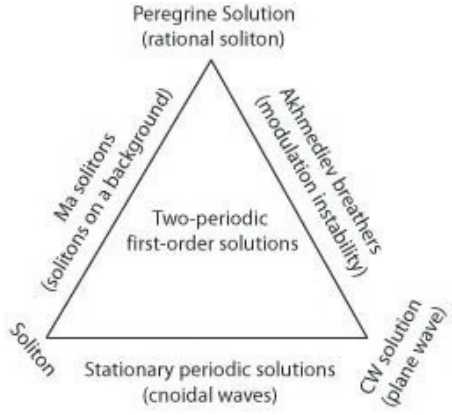

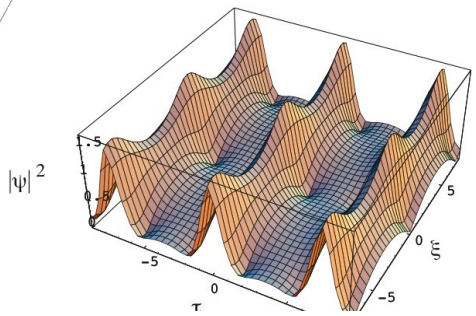

Collision of plain solitons

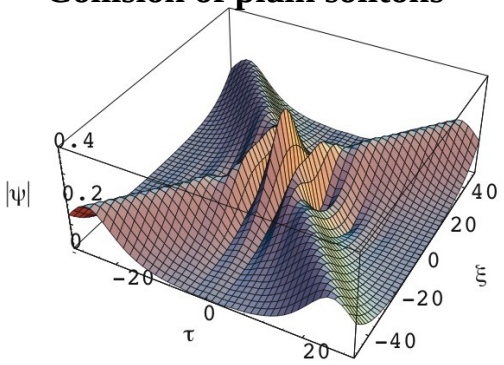

EXACT FIRST-ORDER SOLUTIONS OF THE NONLINEAR SCHRÖDINGER EQUATION

N. N. Akhmediev, V. M. Eleonskii, and
N. E. Kulagin

Translated from Teoreticheskaya i Matematicheskaya Fizika, Vol. 72, No. 2, pp. 183-196, August, 1987. Original article submitted March 12, 1986.

0040-5779/87/7202-0809$12.50

Observation of super-rogue wave

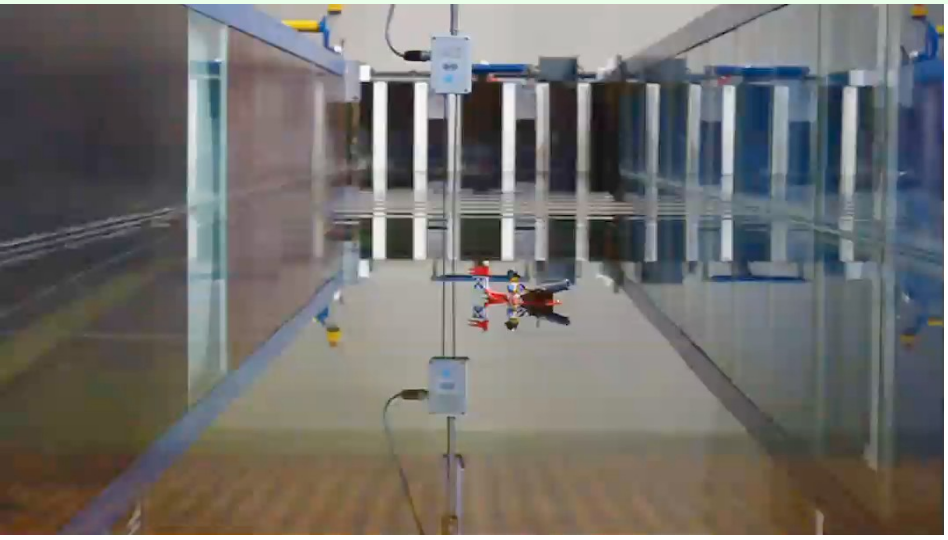

Second order rogue wave:

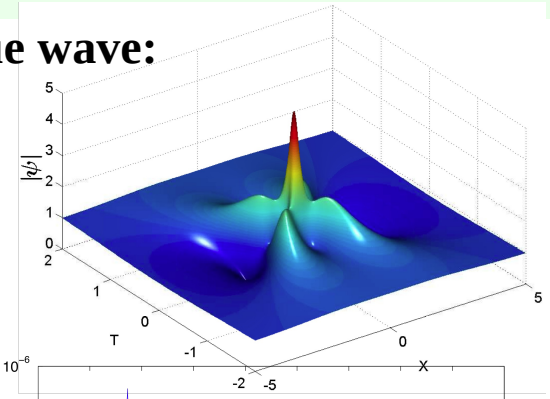

Spectra:

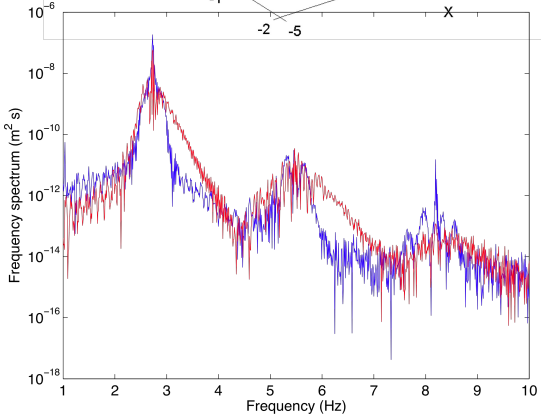

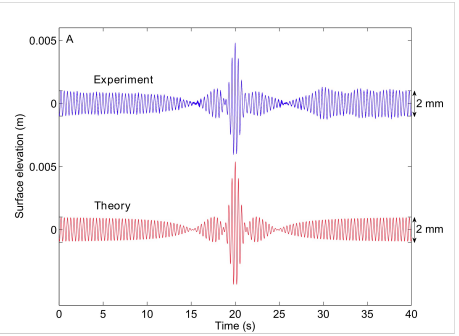

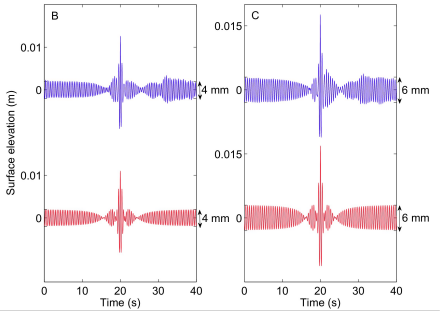

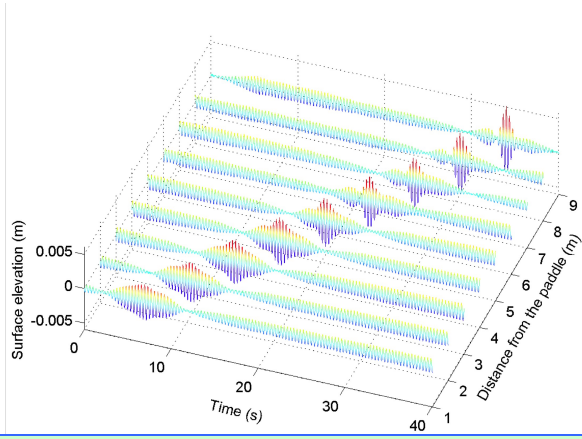

Surface Elevation

Amin Chabchoub et al, PRX (2012)

The Peregrine soliton in nonlinear fibre optics

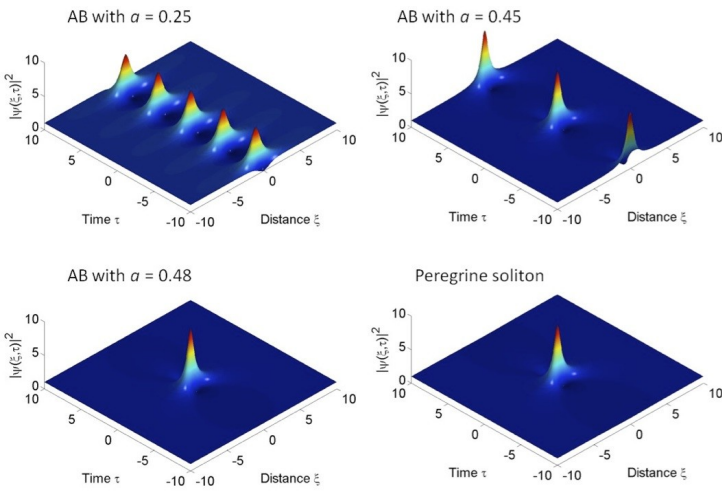

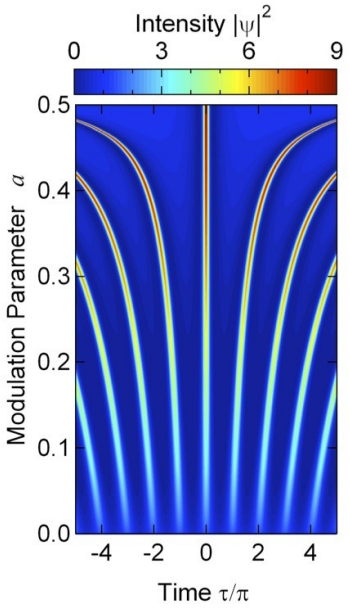

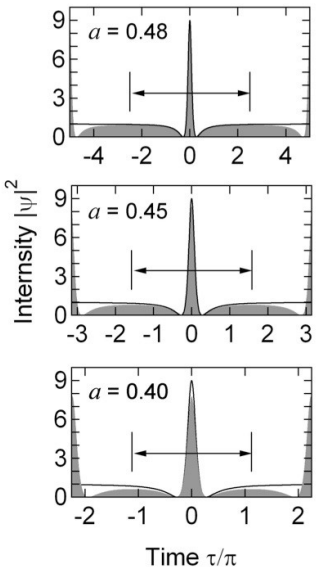

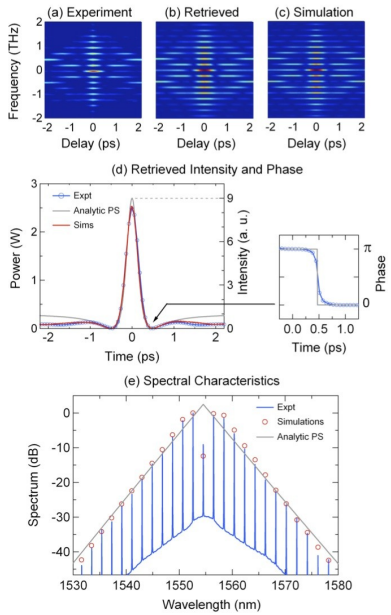

AB solutions with various modulation

parameters a=0.25: 0.45: 0.48 and 0.5

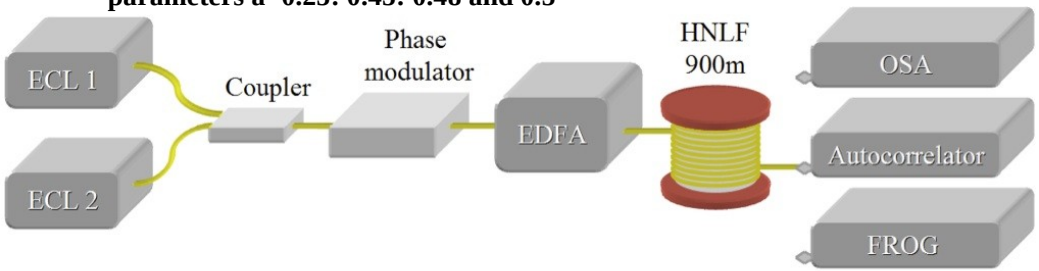

Experimental set-up: ECL: external-cavity laser, OSA: opt. spectrum analyser, HNLF; highly nonlinear fibre, FROG: frequency-resolved opt. gating

Experimental results

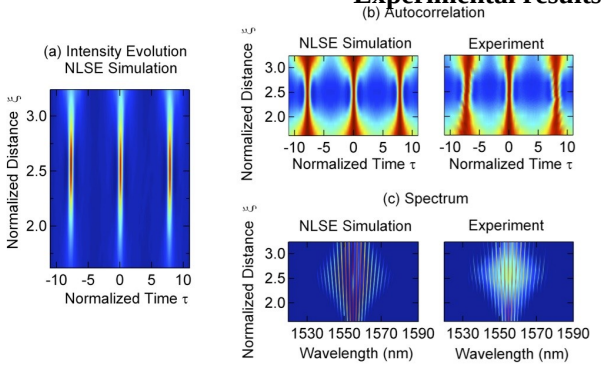

Expected dynamic evolution

B. Kibler et al. Nature Physics, 22 August (2010)

Darboux transformations

$$i\frac{\partial y}{\partial x}+\frac{1}{2}\frac{\partial^2 y}{\partial t^2}+|y|^2 y=0$$

NLSE is a condition of compatibility:

$$R_t = lJR + UR$$

$$R_x = l^2 JR + lUR + \frac{1}{2}VR$$

With the following matrices:

$$U=\begin{pmatrix} 0 & iy^* \\ iy & 0 \end{pmatrix} \quad J=\begin{pmatrix} i & 0 \\ 0 & -i \end{pmatrix}$$

$$V=\begin{pmatrix} -i|y|^2 & y_t^* \\ -y_t & i|y|^2 \end{pmatrix} \quad R=\begin{pmatrix} r \\ s \end{pmatrix}$$

We use the seeding solution of NLSE:

$$\psi_0 = \exp(ix)$$

And obtain the solutions of the linear system:

$$r_1 = \{e^{(2ic_1+ik_1t-ip/2+il_1k_1x)/2} - e^{(-2ic_1-ik_1t+ip/2-il_1k_1x)/2}\}e^{-ix/2}$$

$$s_1 = \{e^{(-2ic_1+ik_1t-ip/2+il_1k_1x)/2} + e^{(2ic_1-ik_1t+ip/2-il_1k_1x)/2}\}e^{ix/2}$$

$$\psi_1 = y_0 + \frac{2(l_1^*-l_1)s_1 r_1^*}{|r_1|^2+|s_1|^2}$$

Eigenvalue is imaginary:

$$l_1 = in_1$$

AB solution:

$$\psi_1 = \left[1-\frac{k_1^2\cosh(d_1x)+2ik_1n_1\sinh(d_1x)}{2(\cosh(d_1x)-n_1\cos(k_1t))}\right]\exp[i(x+p)]$$

$$where \quad d_1 = n_1k_1 \quad and \quad k_1 = 2\sqrt{1-n_1^2}$$

$$r_{12} = \frac{(l_1^*-l_1)s_1^* r_1 s_2 + (l_2-l_1)|r_1|^2 r_2 + (l_2-l_1^*)|s_1|^2 r_2}{|r_1|^2+|s_1|^2}$$

$$s_{12} = \frac{(l_1^*-l_1)s_1 r_1^* r_2 + (l_2-l_1)|s_1|^2 s_2 + (l_2-l_1^*)|r_1|^2 s_2}{|r_1|^2+|s_1|^2}$$

Higher order solution:

$$\psi_2 = y_1 + \frac{2(l_2^*-l_2)s_{12}r_{12}^*}{|r_{12}|^2+|s_{12}|^2}$$

Collision of breathers

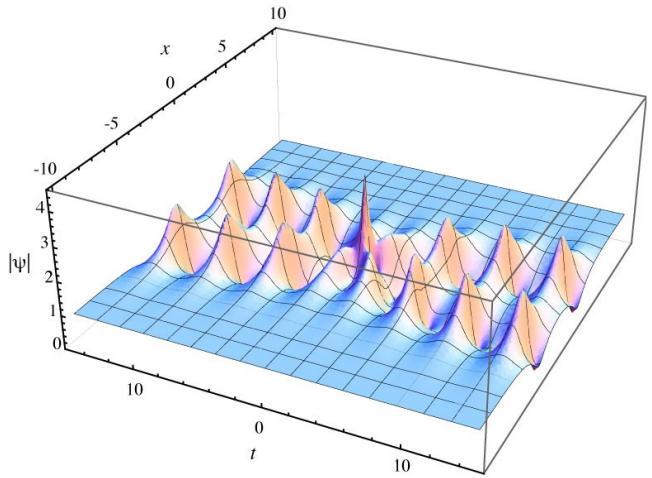

Collision of two ABs with zero velocity

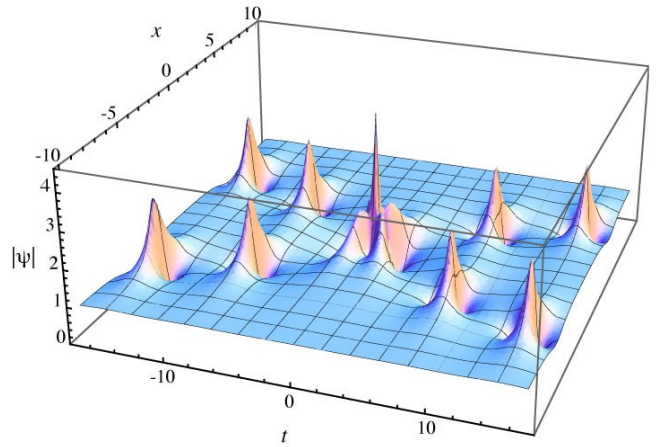

Collision of two ABs with nonzero velocity

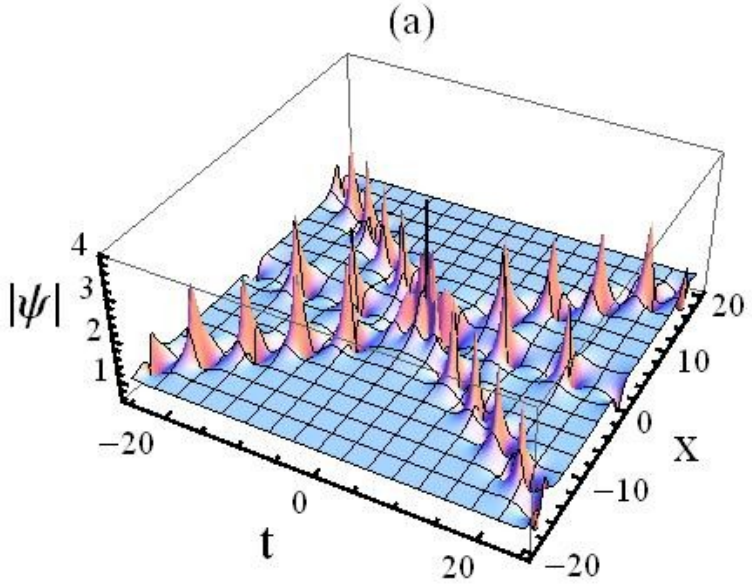

Collision of 3 ABs with eigenvalues:

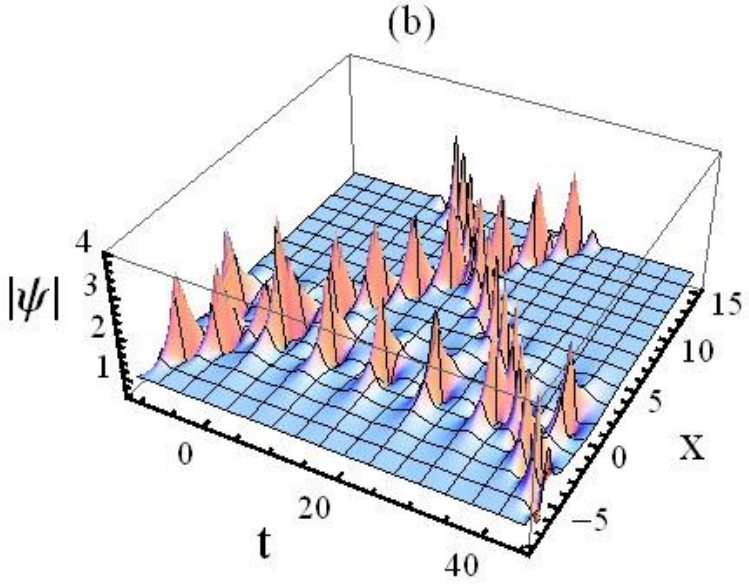

Collision of 3 ABs with eigenvalues:

Waves that appear from nowhere and disappear without a trace

$$i\frac{\partial y}{\partial x}+\frac{1}{2}\frac{\partial^2 y}{\partial t^2}+|y|^2 y=0$$

First order rational solution:

$$\psi=\left[1-4\frac{1+2ix}{1+4x^2+4t^2}\right]\exp(ix)$$

Higher order rational solution:

$$\psi=\left[1-\frac{G+iH}{D}\right]\exp(ix)$$

$$G=-\frac{3}{16}+\frac{3}{2}t^2+t^4+\frac{9}{2}x^2+6t^2x^2+5x^4$$

$$=\left(t^2+x^2+\frac{3}{4}\right)\left(t^2+5x^2+\frac{3}{4}\right)-\frac{3}{4}$$

$$H=-\frac{15}{8}x-3t^2x+2t^4x+x^3+4t^2x^3+2x^5=$$

$$=x\left[x^2-3t^2+2\left(t^2+x^2\right)^2-\frac{15}{8}\right]$$

$$D=\frac{3}{64}+\frac{9t^2}{16}+\frac{t^4}{4}+\frac{t^6}{3}+\frac{33}{16}x^2$$

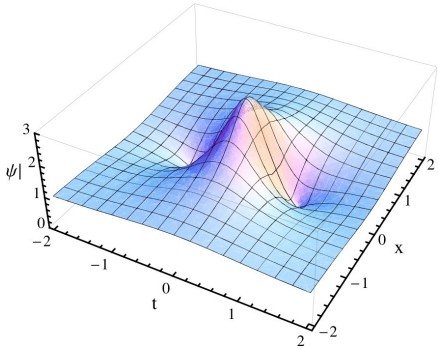

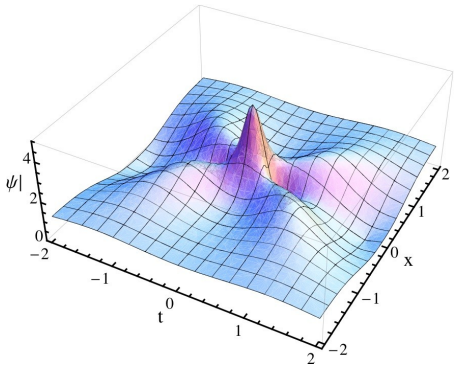

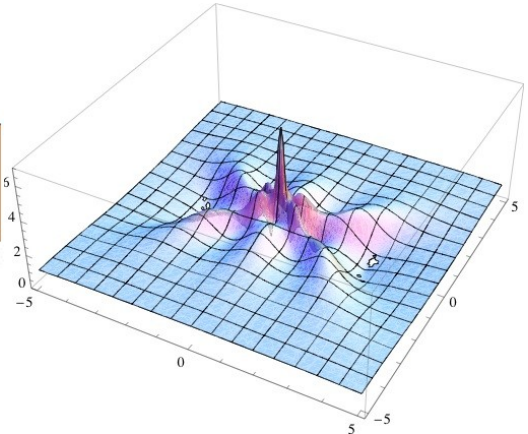

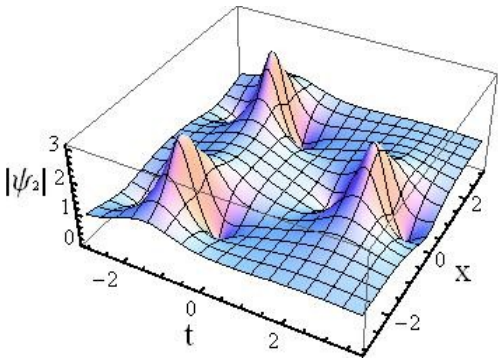

Physics Letters A 373 (2009) 675–678

Contents lists available at ScienceDirect

Physics Letters A

www.elsevier.com/locate/pla

Waves that appear from nowhere and disappear without a trace

N. Akhmediev [a], A. Ankiewicz [a,*], M. Taki [b]

[a] Optical Sciences Group, Research School of Physics and Engineering, The Australian National University, Canberra ACT 0200, Australia
[b] Laboratoire de Physique des Lasers, Atomes et Molécules, UMR CNRS 8523, Centre d'Études et de Recherches Lasers et Applications, Université des Sciences et Technologies de Lille, 59655 Villeneuve d'Ascq Cedex, France

Higher-order translations

AB solution: $l = i\,0.65$

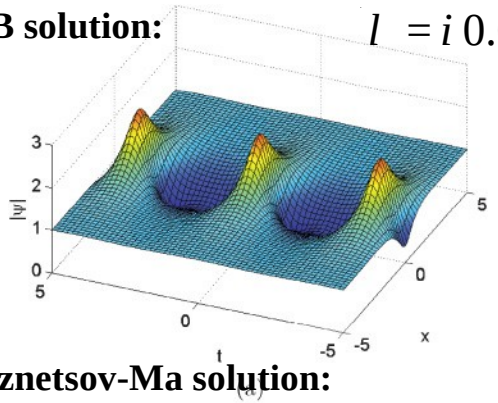

Kuznetsov-Ma solution: $l = i\,1.35$

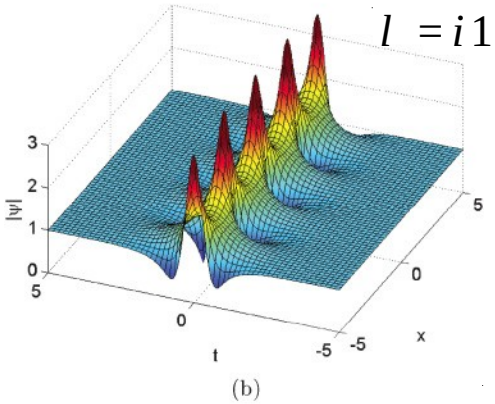

(b)

Peregrine solution: $l = i$

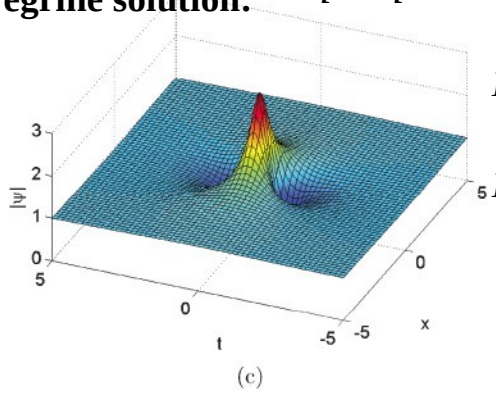

(c)

Shifts:

$$x_j = X_{j1} + X_{j2}k^2 + X_{j3}k^4 + \ldots$$
$$t_j = T_{j1} + T_{j2}k^2 + T_{j3}k^4 + \ldots$$

Modulation frequencies:

$$\kappa = 2\sqrt{1 + l_j^2}$$

In the first order case, n=1:

$$G_1 = 4$$
$$H_1 = 8(x - X_{11})$$
$$D_1 = 1 + 4(x - X_{11})^2 + 4(1 - T_{11})^2$$

In the second order case, n=2:

$$G_2 = -\frac{1}{8}(5x^2 + t^2)(x^2 + t^2) - \frac{3}{16}(3x^2 + t^2) + xx_d + tt_d + \frac{3}{128}$$

$$H_{21} = -\frac{1}{4}x(x^2 + t^2)^2 - \frac{1}{8}x(x^2 - 3t^2) + \frac{15}{64}x + \left(x^2 - t^2 - \frac{1}{4}\right)x_d + 2xtt_d$$

$$D_2 = \frac{1}{24}(x^2 + t^2)^3 + \frac{1}{32}(3x^2 - t^2)^2 + \frac{3}{128}(11x^2 + 3t^2) + \frac{3}{512}$$
$$- \left(\frac{1}{3}x^3 - xt^2 + \frac{3}{4}x - \frac{2}{3}x_d\right)x_d - \left(x^2t - \frac{1}{3}t^3 + \frac{1}{4}t - \frac{2}{3}t_d\right)t_d$$

$$\psi_n(x,t) = \left[(-1)^n + \frac{G_n + iH_n}{D_n}\right]e^{ix}$$

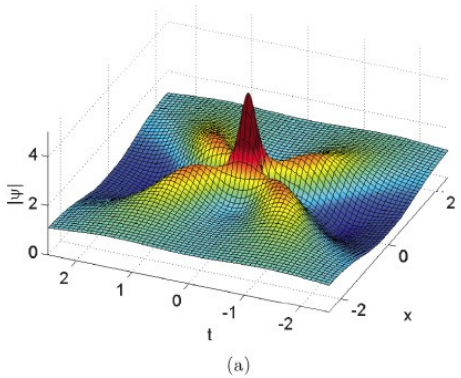

(a)

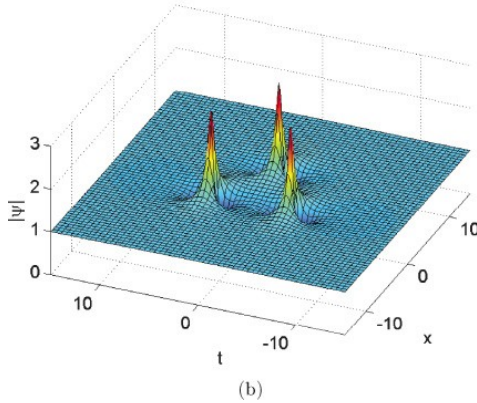

(b)

$$x_d = X_{12} - X_{22}$$
$$t_d = T_{12} - T_{22}$$

$$R \approx 2^{2/3}(x_d^2 + t_d^2)^{1/6}$$

Kedziora, PR E 84, 056611 (2011)

Infinite period limit of ABs

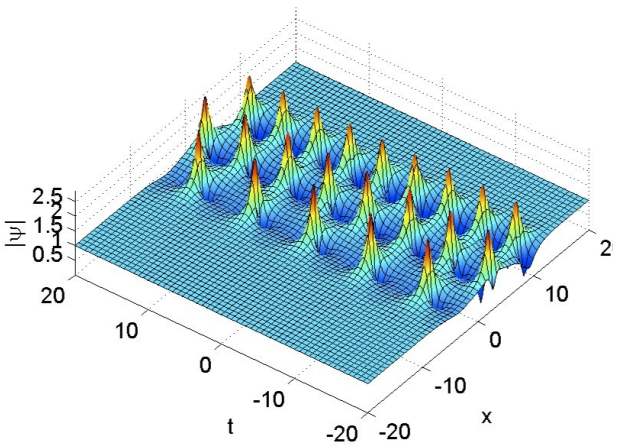

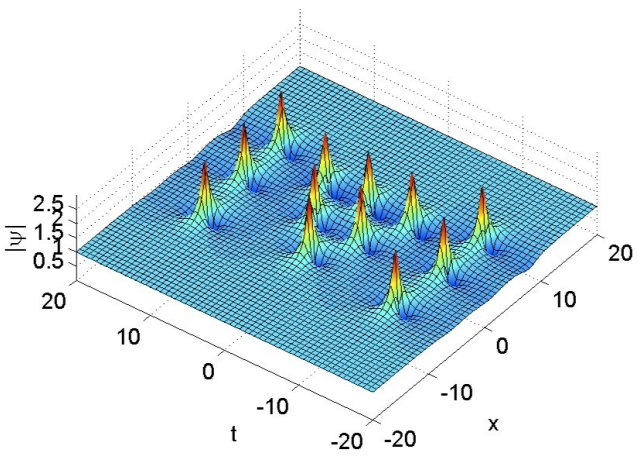

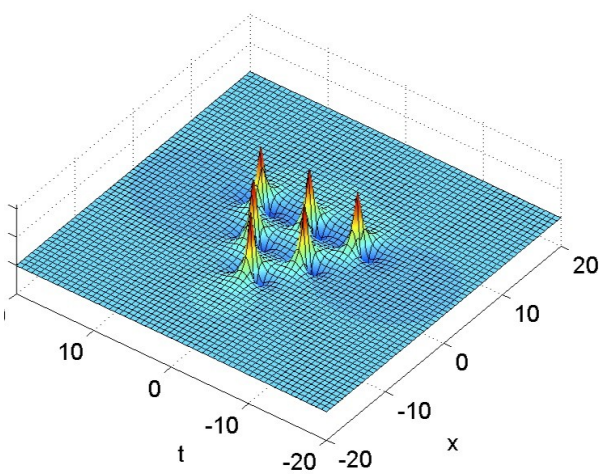

$\kappa_1 = k, \quad k_2 = \sqrt{2}k, \quad k_3 = \sqrt{3}k,$

$x_1 = 0\,k^2 \quad x_2 = 5k^2 \quad x_3 = 10k^2$

$(a) \quad k = 0.8, \quad (b) \quad k = 0.5, \quad (c) \quad k \to 0,$

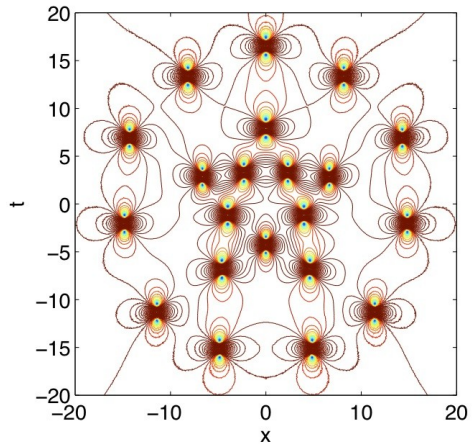

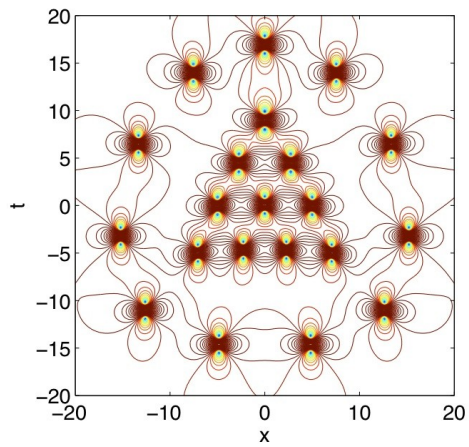

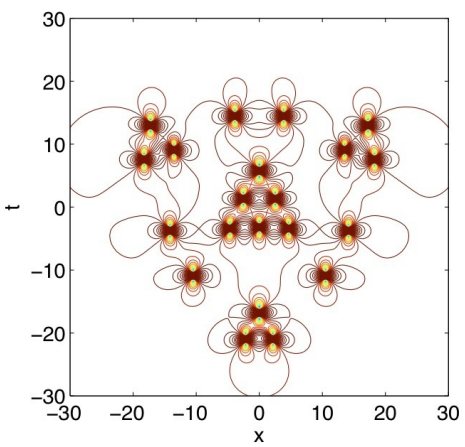

Rogue wave clusters

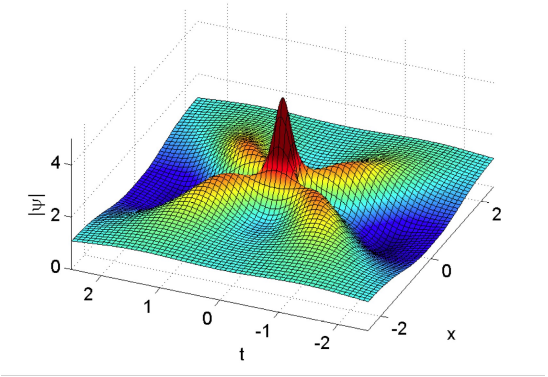

N=2

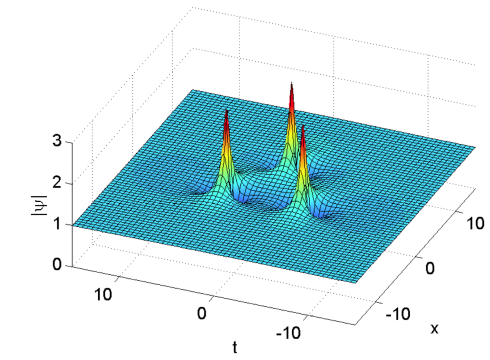

Rogue wave of order n:

Total number of PS in the structure n(n+1)/2

Order of the central peak n-2, Number of PS in the circular shell 2n-1

N=3

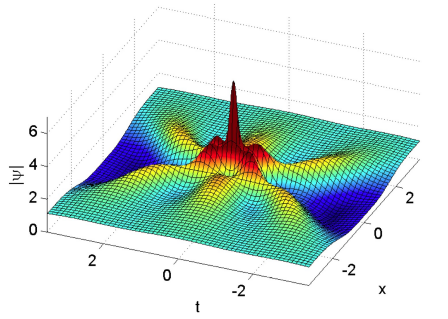

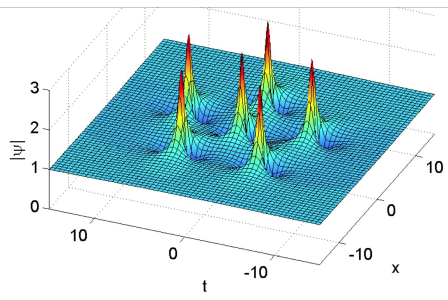

N=4

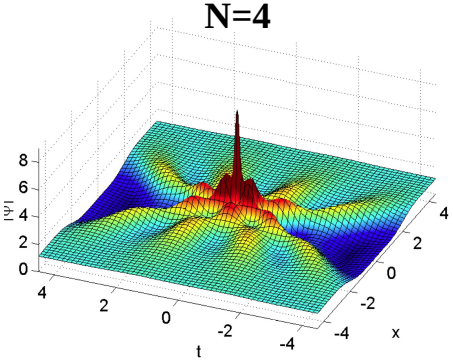

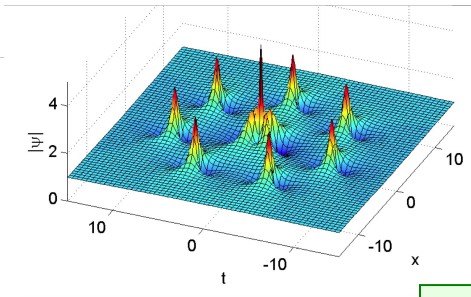

N=5

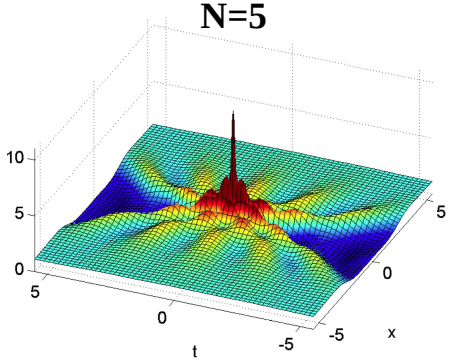

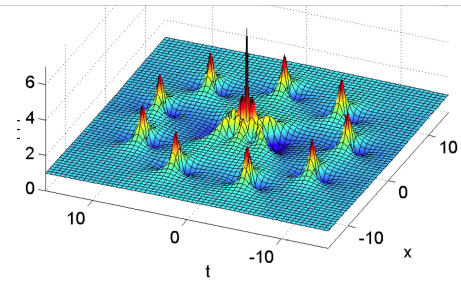

N=8

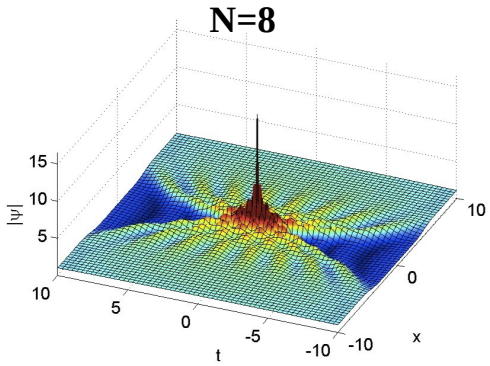

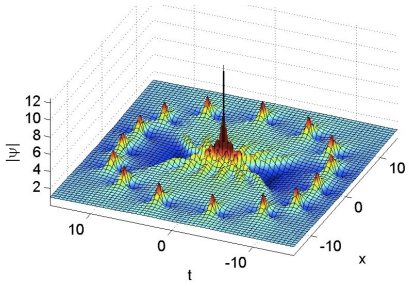

Kedziora et al, Phys. Rev. E 84, 056611 (2011)

Astronomers capture death of star

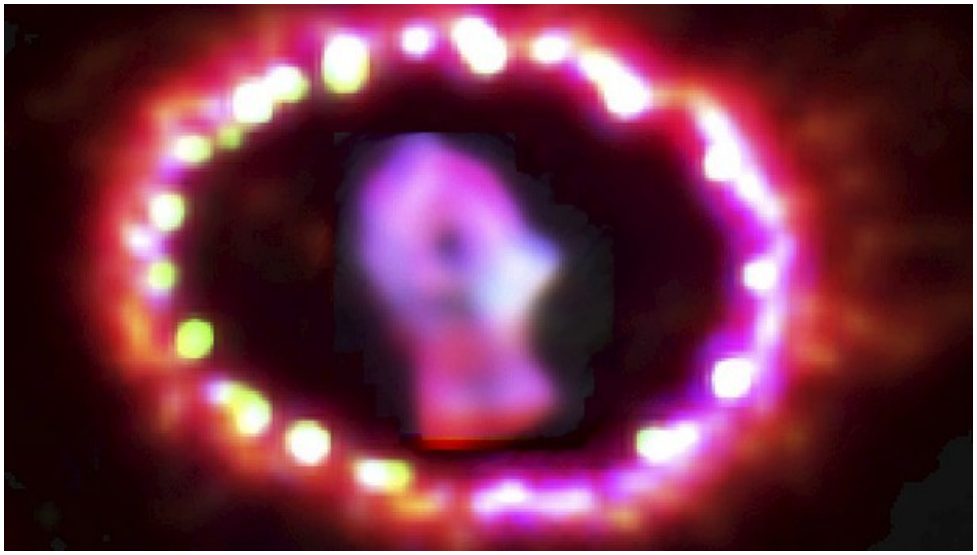

The 1987A supernova

April 3, 2013

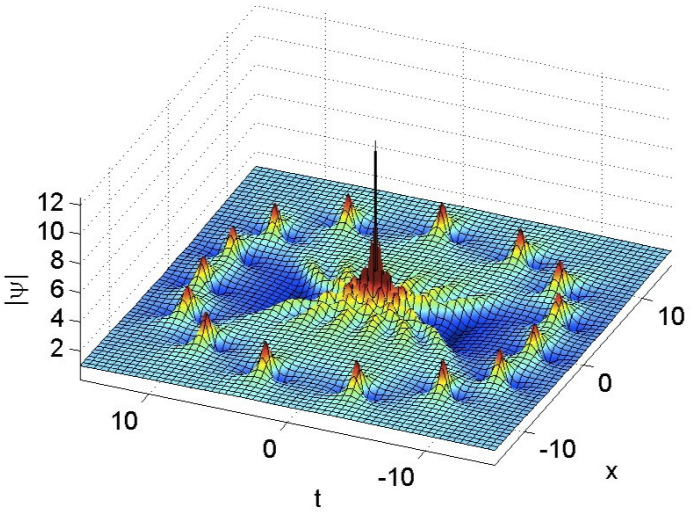

The ring consists of 19 RWs. (2N-1)=19. Thus N=10

Scientists in Australia have captured the most detailed images yet of the death of a giant star. A team of astronomers led by the International Centre for Radio Astronomy Research (ICRAR) in Western Australia has revealed new images of the death throes of Supernova 1987A, whose demise was first spotted more than 25 years ago. Situated on the outskirts of the Tarantula Nebula in the Large Magellanic Cloud, SN1987A expired about 168,000 light years from Earth.

In new research published in the Astrophysical Journal, a team of astronomers from Australia and Hong Kong has succeeded in using the Australia Telescope Compact Array, a CSIRO radio telescope in NSW, to make the highest-resolution images yet of the expanding supernova.

Rogue wave cascades

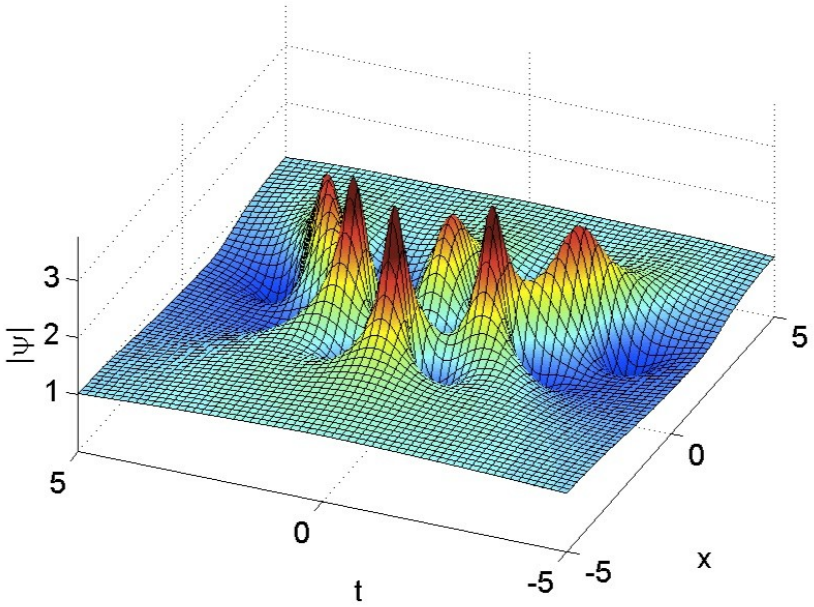

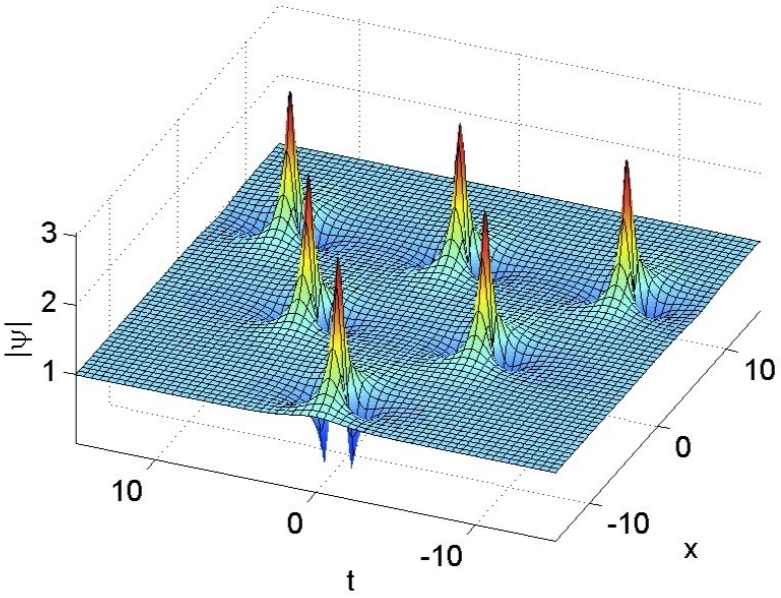

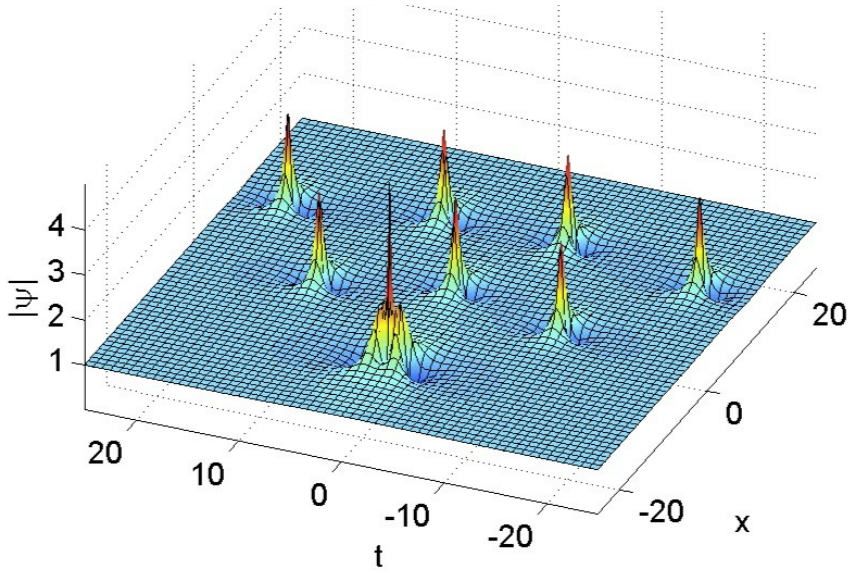

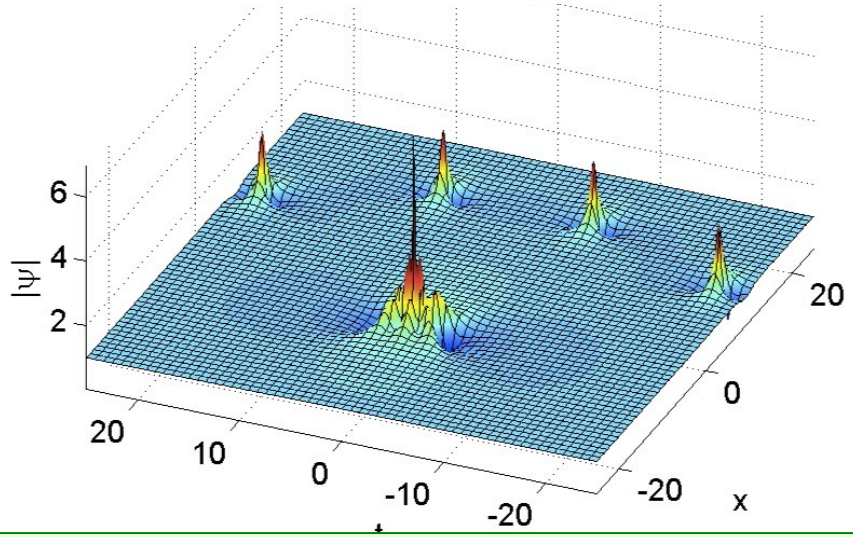

Kedziora et al, Phys. Rev. E 84, 056611 (2011)

Higher order modulation instability

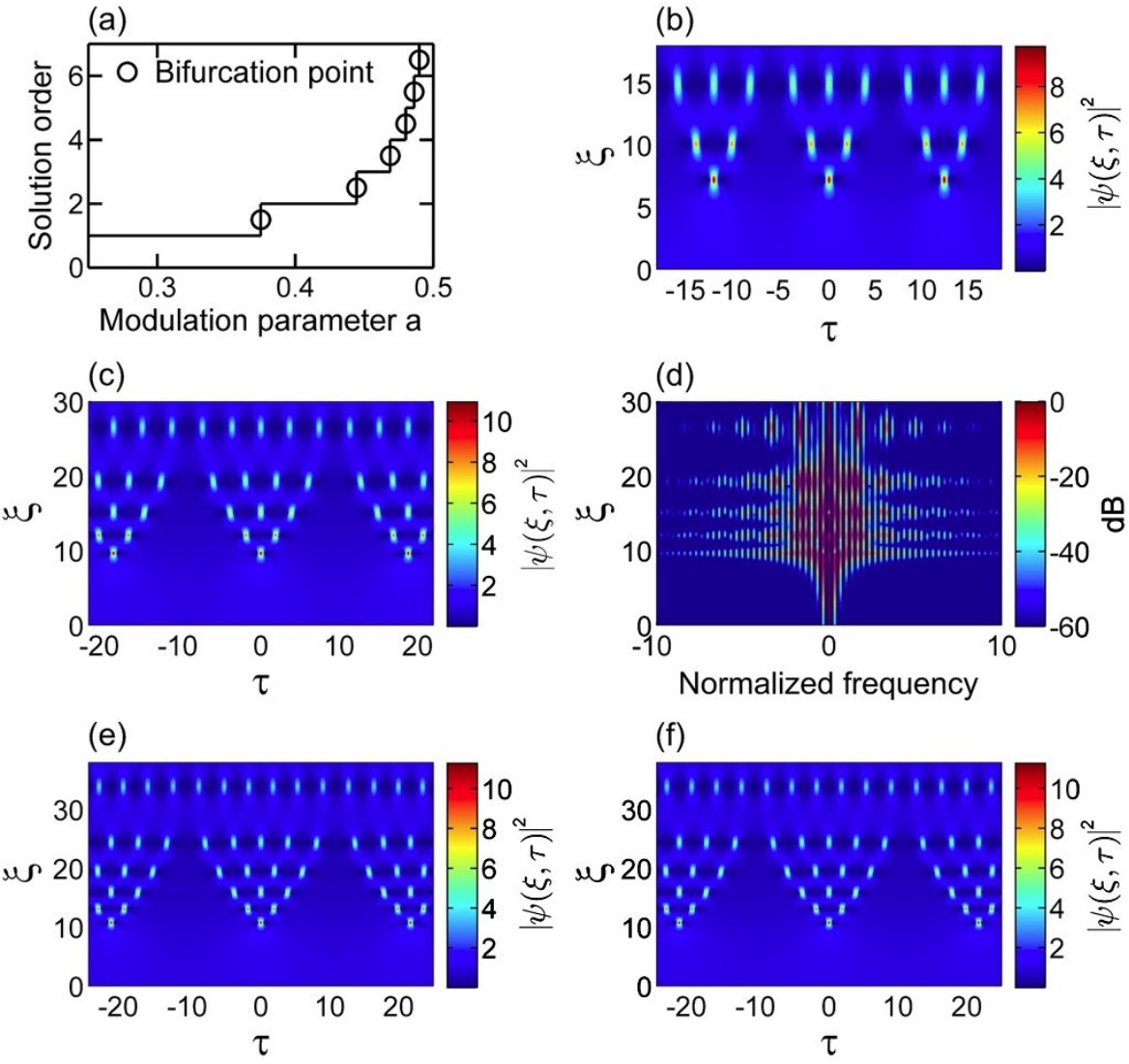

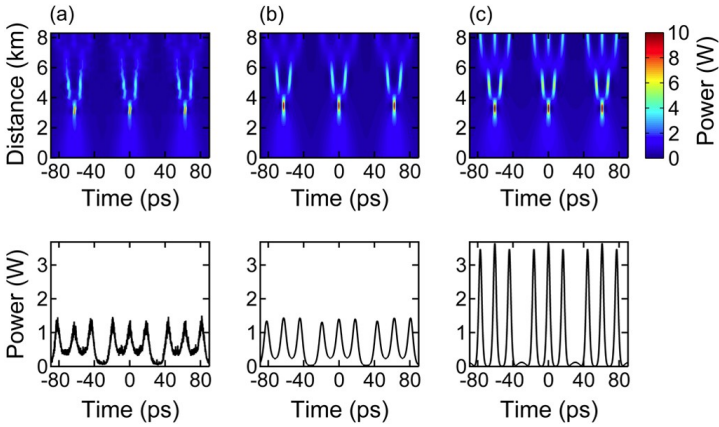

Erkintalo et al, Phys. Rev. Lett., 107, 253901 (2011)

Classification of higher order rogue wave structures

S. O.	Qu.	SA1	SA2	SA3	SA4	SA5
0	0	**0**	$3\times0+\mathbf{0}$	$5\times0+\mathbf{0}$	$7\times0+\mathbf{0}$	$9\times0+\mathbf{0}$
1	1	**1**	$3\times0+\mathbf{1}$	$5\times0+\mathbf{1}$	$7\times0+\mathbf{1}$	$9\times0+\mathbf{1}$
2	3	**3**	$3\times1+\mathbf{0}$	$5\times0+\mathbf{3}$	$7\times0+\mathbf{3}$	$9\times0+\mathbf{3}$
3	6	**6**	$3\times2+\mathbf{0}$	$5\times1+\mathbf{1}$	$7\times0+\mathbf{6}$	$9\times0+\mathbf{6}$
4	10	**10**	$3\times3+\mathbf{1}$	$5\times2+\mathbf{0}$	$7\times1+\mathbf{3}$	$9\times0+\mathbf{10}$
5	15	**15**	$3\times5+\mathbf{0}$	$5\times3+\mathbf{0}$	$7\times2+\mathbf{1}$	$9\times1+\mathbf{6}$
6	21	**21**	$3\times7+\mathbf{0}$	$5\times4+\mathbf{1}$	$7\times3+\mathbf{0}$	$9\times2+\mathbf{3}$
7	28	**28**	$3\times9+\mathbf{1}$	$5\times5+\mathbf{3}$	$7\times4+\mathbf{0}$	$9\times3+\mathbf{1}$
8	36	**36**	$3\times12+\mathbf{0}$	$5\times7+\mathbf{1}$	$7\times5+\mathbf{1}$	$9\times4+\mathbf{0}$
9	45	**45**	$3\times15+\mathbf{0}$	$5\times9+\mathbf{0}$	$7\times6+\mathbf{3}$	$9\times5+\mathbf{0}$
10	55	**55**	$3\times18+\mathbf{1}$	$5\times11+\mathbf{0}$	$7\times7+\mathbf{6}$	$9\times6+\mathbf{1}$
…	…	…	…	…	…	…

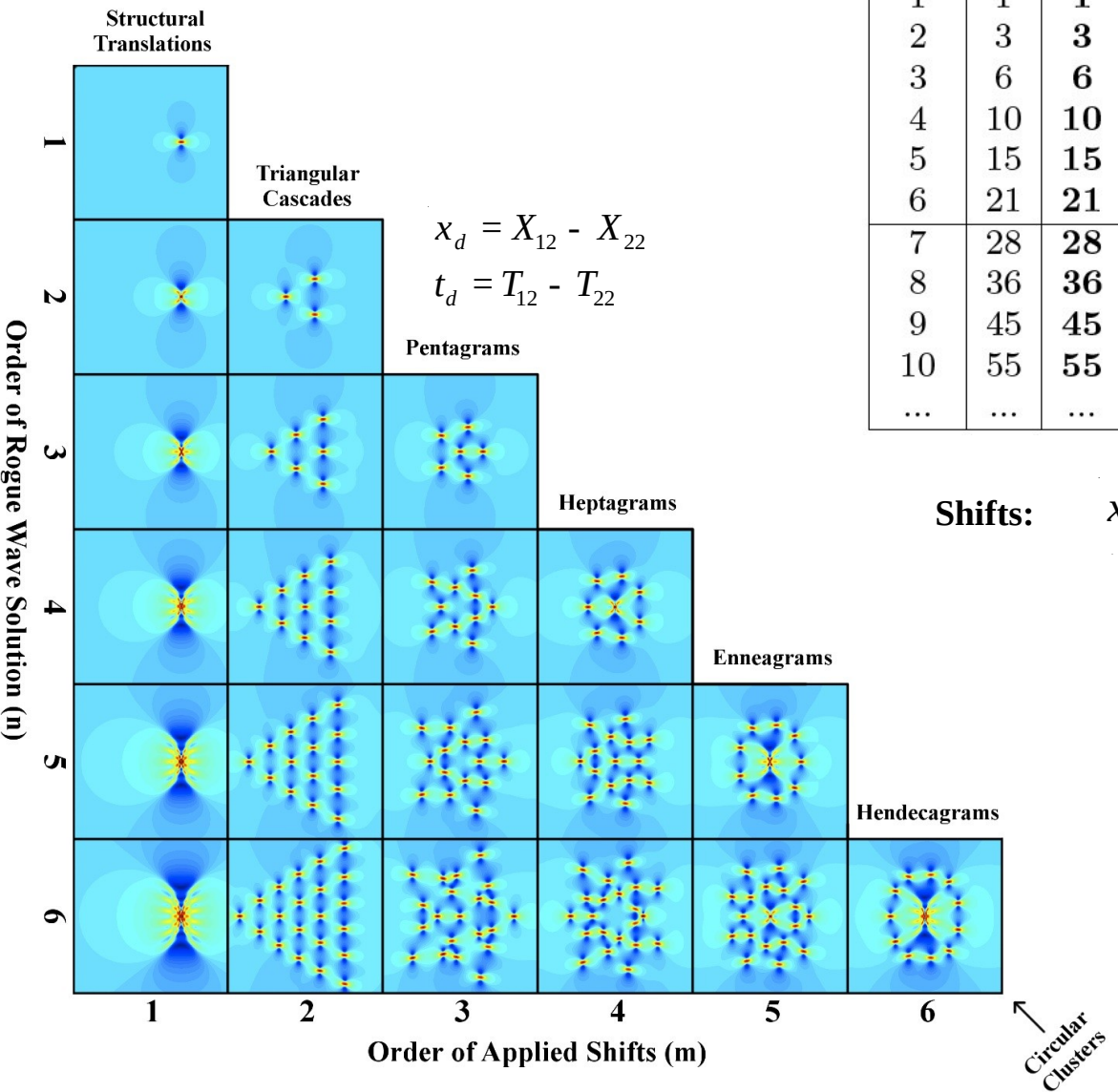

Shifts: $x_j = X_{j1} + X_{j2}k^2 + X_{j3}k^4 + X_{j4}k^6 + ..$

$t_j = T_{j1} + T_{j2}k^2 + T_{j3}k^4 + T_{j3}k^5 + ..$

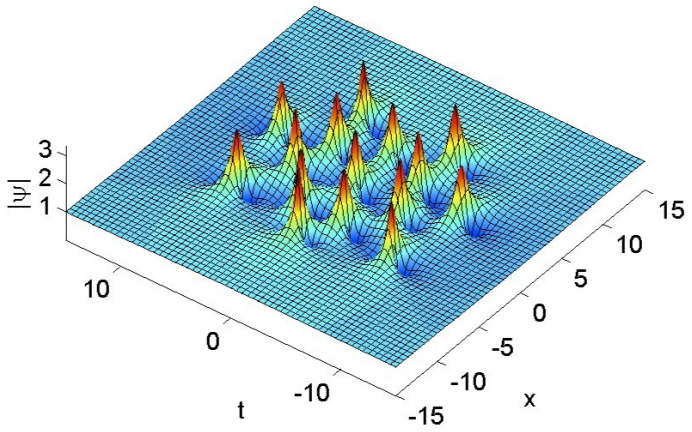

Rogue waves of Hirota equation

$$iy_x + \frac{1}{2}y_{tt} + |y|^2 y = ie[y_{ttt} + 6|y|^2 y_t]$$

Very little difference from the NLSE case

First order rogue wave:

$$\psi = \left[1 - \frac{4(1+2ix)}{1+4(t+6ex)^2+4x^2}\right]\exp(ix)$$

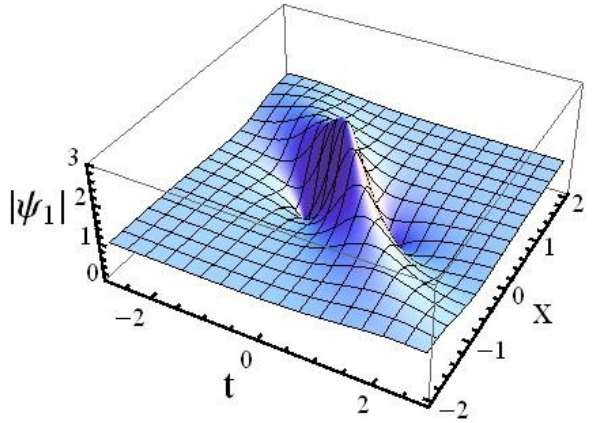

Second order rogue wave:

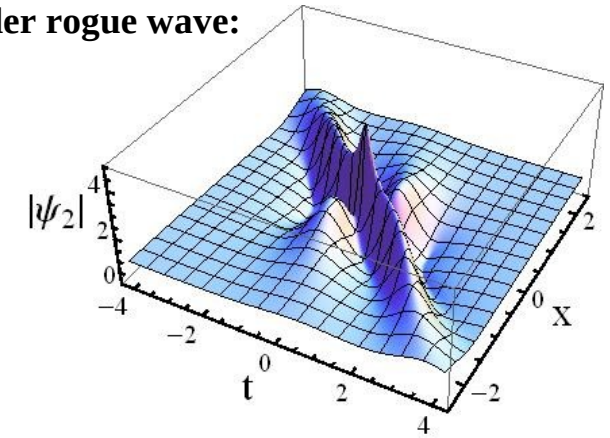

Breather solution:

$$\psi = \left[\frac{2(1-2a_1)Cosh(bx) + ib\,Sinh(bx)}{Cosh(bx) - \sqrt{2a_1}Cos[s(t+vx)]} - 1\right]\exp(ix)$$

where $s = 2\sqrt{1-2a_1}$, $b = \sqrt{2a_1}\,s$ *and* $v = 2e(1+4a_1)$

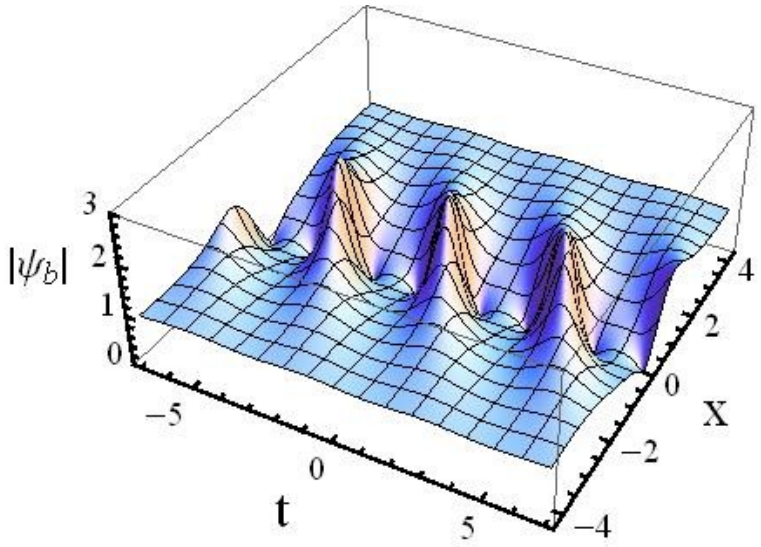

Ankiewicz et al, PRE 81, 046602 (2010)

Rogue waves of the Sasa-Satsuma equation

$$iy_t + \frac{1}{2}y_{xx} + |y|^2 y = ie\left[y_{xxx} + 3(|y|^2)_x y + 6|y|^2 y_x\right]$$

Modulation instability of a plane wave:

$$\psi_0 = -\frac{c}{2e}\exp\left[i\left(\frac{k}{2e}x + \frac{w}{8^2}t\right)\right] \qquad \omega = 2c^2 - k^2 + (6kc^2 - k^3)$$

$$\psi = \psi_0(1 + A\exp[ik(x - Wt)] + B^*\exp[-ik(x - Wt)])$$

Growth rate of modulation instability:

$$\gamma = \pm\frac{\kappa}{4e}\sqrt{4(3k+1)^2(c^2 - k^2e^2) - 9c^4}$$

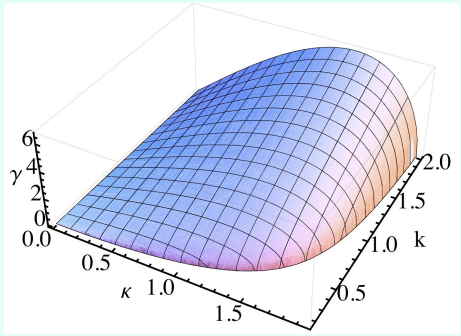

Three parameters control the solution: $c = 1,\quad e = 0.5\quad k = 0.8$

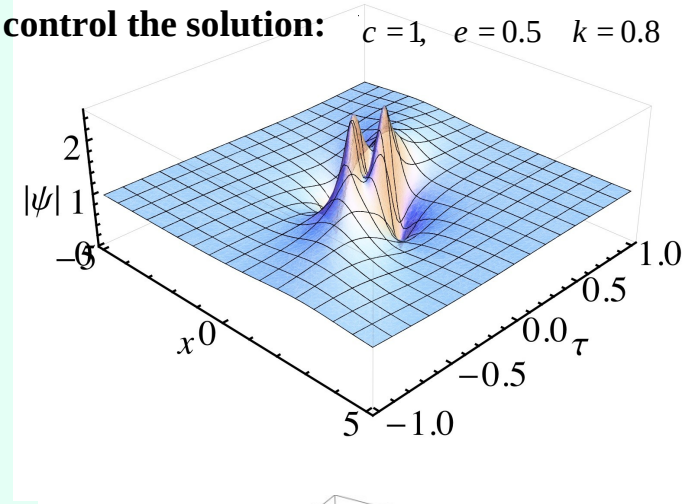

Rogue wave solution:

$$\psi = -\frac{c}{2e}\left(1 - \frac{z - z^*}{c}\frac{G}{\psi}\right)\exp\left[i\left(\frac{k}{2e}x + \frac{w}{8^2}t\right)\right]$$

$$G = \frac{|u|^2\,\mathrm{Re}z(zu^*g + z^*uh^*) + (z|g|^2 + z^*|h|^2)(z^*u^*g + zuh^*)}{|z|^2(|u|^2 + |g|^2 + |h|^2)^2 - |u^2 + 2hg|^2(\mathrm{Im}z)^2}$$

Variables x and τ enter here:

$$u = \left(\frac{v_{21}}{2}t - 2ex\right)$$

$$v_{21} = \pm\frac{9(a - 6c^2)z^4 + 3a(a - 1 - 18c^2)z^2 + a^3}{3(2z^2 + dz + a)^2}$$

$$h = 3c\left(\frac{u}{M_1} + i\frac{12e^2}{M_1^2}\right) \qquad M_1 = K + d - z$$

$$g = 3c\left(\frac{u}{M_2} - i\frac{12e^2}{M_2^2}\right) \qquad M_2 = K - d + z$$

$$K = 3k + 1$$

Eigenvalue of scattering problem:

$$\zeta = \pm\frac{i\sqrt{9c^2(9c^2 + 10K^2) + 3c(9c^2 + 4K^2)^{3/2} - 2K^4}}{3\sqrt{2}K}$$

$$d = \left(\frac{b}{2} + \frac{2(K^2 + 18c^2 + 3z^2)}{3b}\right) \qquad a = \frac{(K^2 - 3 - 36c^2)}{3} \qquad b = (-1 + i\sqrt{3})[(K^2 - 9c^2 - z^2)z]^{1/3}$$

$c = 1,\quad e = 0.5\quad k = 2$

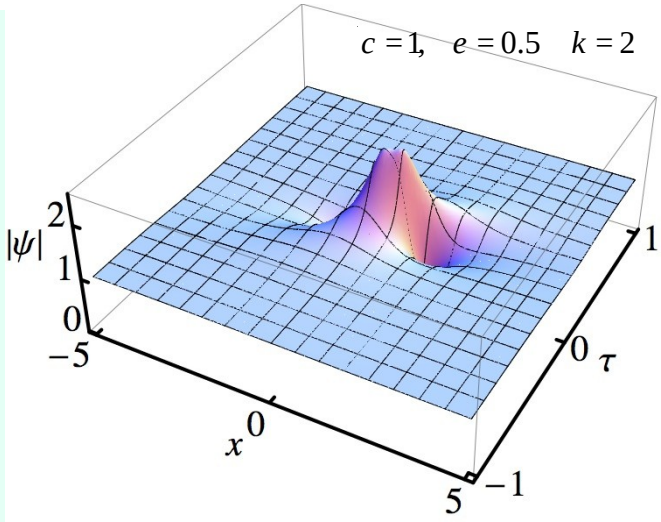

Physics Letters A **376**, 1558 (2012)

First order rational solution

$$i\frac{\partial y}{\partial x}+\frac{1}{2}\frac{\partial^2 y}{\partial t^2}+|y|^2 y=0$$

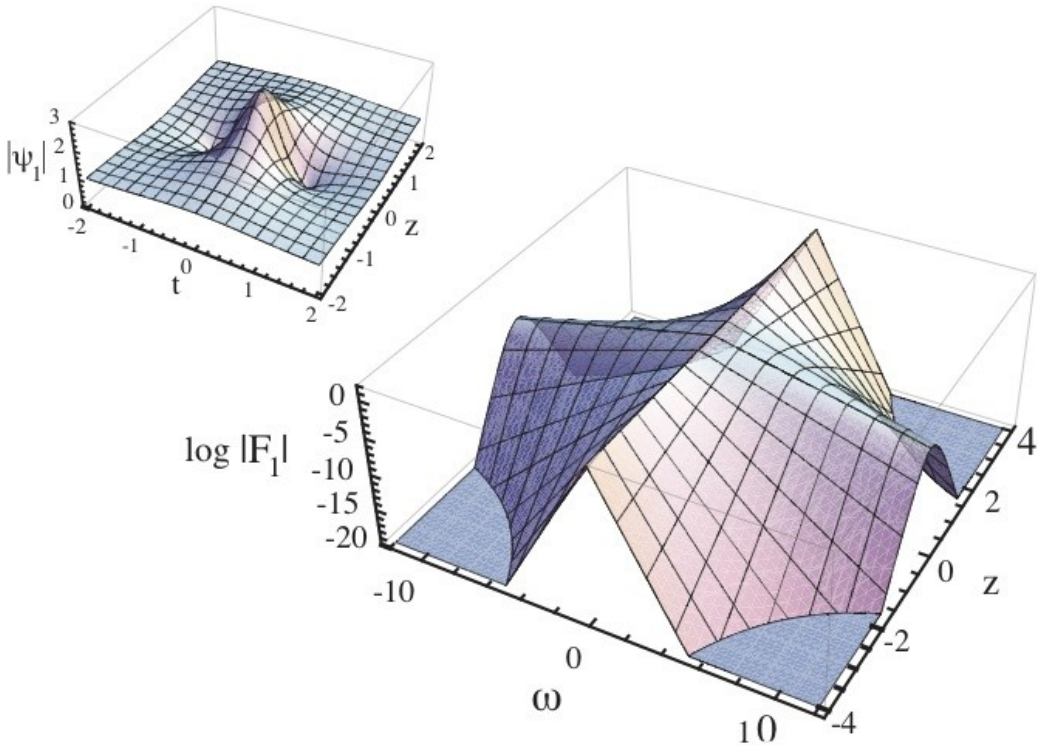

First order rational solution:

$$\psi=\left[1-4\frac{1+2ix}{1+4x^2+4t^2}\right]\exp(ix)$$

Its spectrum:

$$F(w,z)=$$

$$=\frac{1}{\sqrt{2p}}\int_{-\infty}^{\infty}u(z,t)e^{iwt}dt=$$

$$=\sqrt{2p}\left[\frac{1+2iz}{\sqrt{1+4z^2}}\exp\left(-\frac{|w|}{2}\sqrt{1+4z^2}\right)-d(w)\right]\exp(iz)$$

Modulus:

$$|F(w,z)|=\sqrt{2p}\exp\left(-\frac{|w|}{2}\sqrt{1+4z^2}\right)$$

Second order rational solution

$$i\frac{\partial y}{\partial x}+\frac{1}{2}\frac{\partial^2 y}{\partial t^2}+|y|^2 y=0$$

Second order rational solution:

$$\psi=\left[1-\frac{G+iH}{D}\right]\exp(ix)$$

$$G=-\frac{3}{16}+\frac{3}{2}t^2+t^4+\frac{9}{2}x^2+6t^2x^2+5x^4$$

$$=\left(t^2+x^2+\frac{3}{4}\right)^2+5x^2+\frac{3}{4}-\frac{3}{4}$$

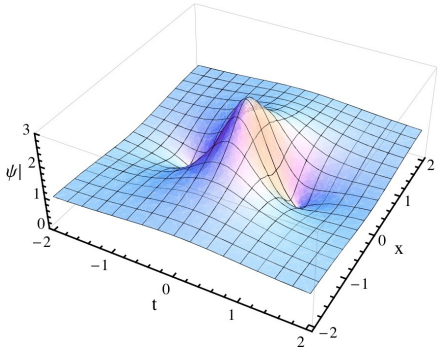

$$H=-\frac{15}{8}x-3t^2x+2t^4x+x^3+4t^2x^3+2x^5=$$

$$=x\left[x^2-3t^2+2\left(t^2+x^2\right)^2-\frac{15}{8}\right]$$

The spectrum of the second order solution:

$$D=\frac{3}{64}+\frac{9t^2}{16}+\frac{t^4}{4}+\frac{t^6}{3}+\frac{33}{16}x^2$$

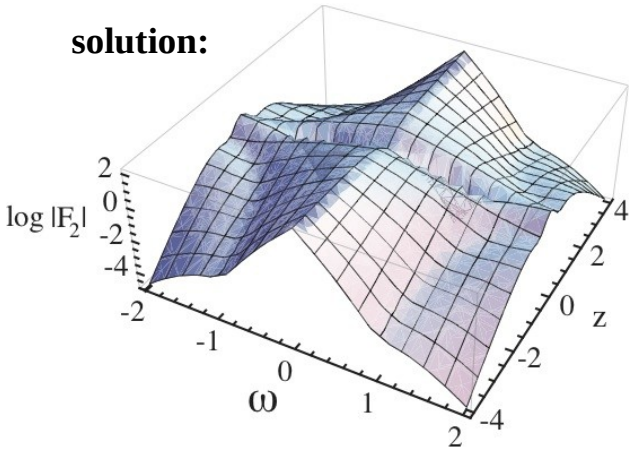

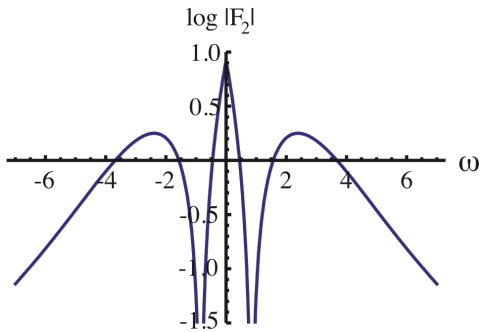

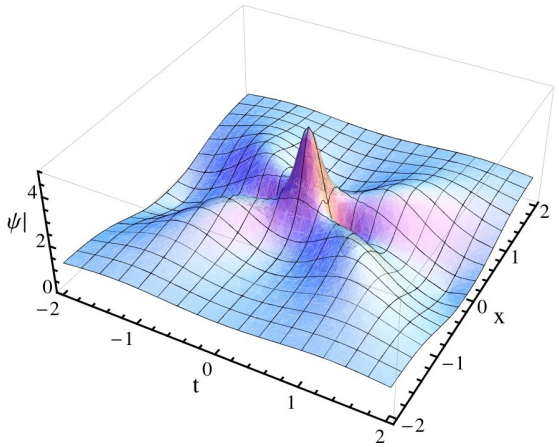

Early detection of rogue waves in a chaotic wave field

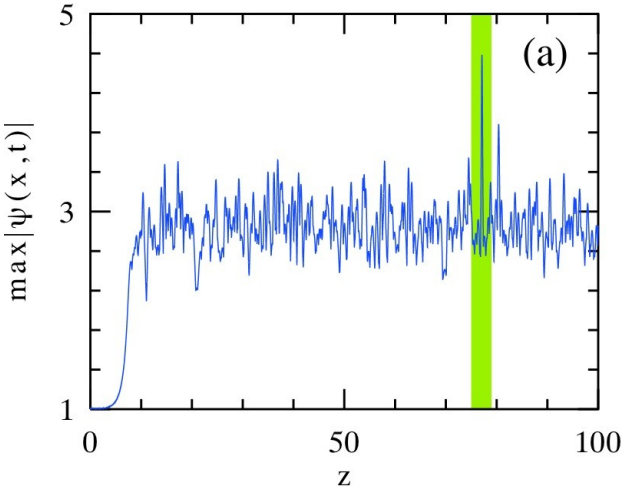

Evolution of maxima of the chaotic field generated from the CW background

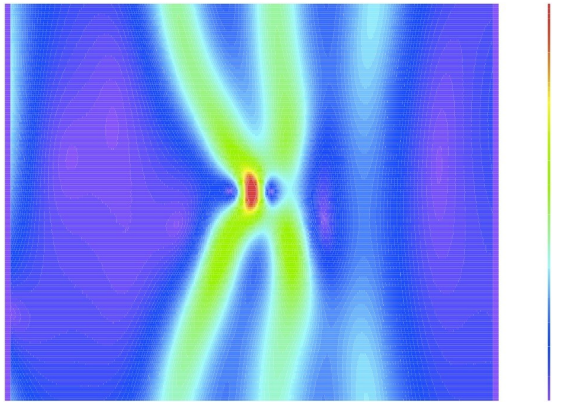

Contour plot of the chaotic field around the rogue wave

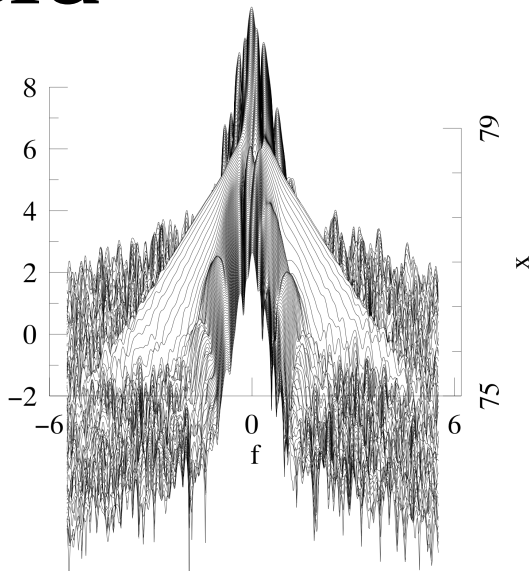

Evolution of the spectrum for the same rogue wave

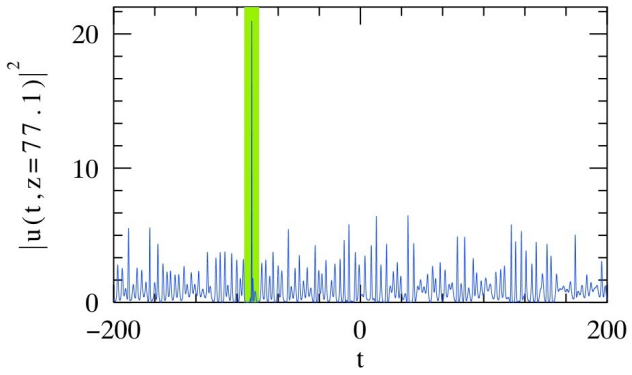

The total t-window of the chaotic field where the rogue wave appears

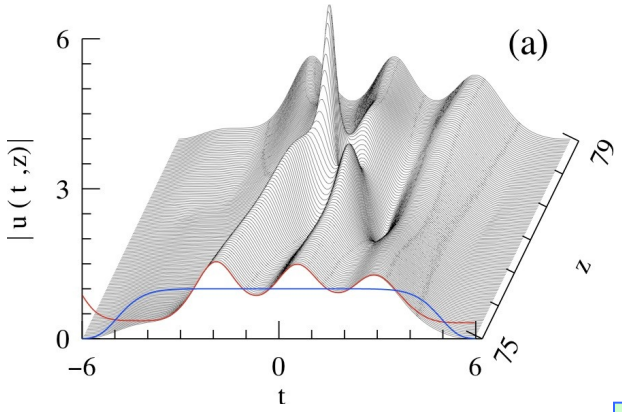

3D plot of the same rogue wave

PLA 375, 2999 (2011)

Dissipative rogue waves: model

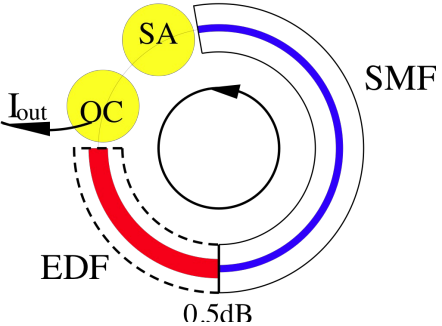

Model of the fiber laser

Transfer function of saturable absorber:

$$T = T_0 + \Delta T \frac{I(t)}{I_{sat} + I(t)} \quad where \quad I(t) = |\psi(t)|^2$$

A dissipative system is the one with continuous pump and losses in the Sense introduced by Prigogine. In other words, it is a system far from equilibrium.

A few samples of output radiation

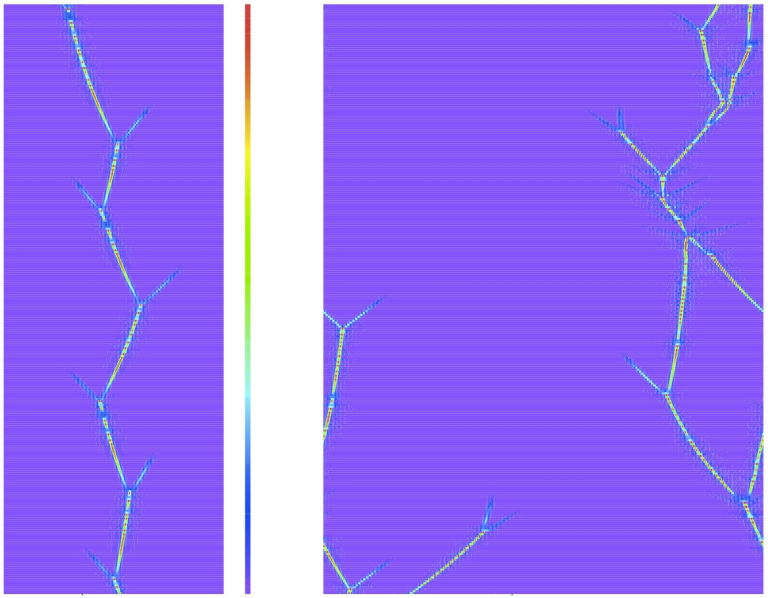

$Q_{sat} = 3$

$Q_{sat} = 6$

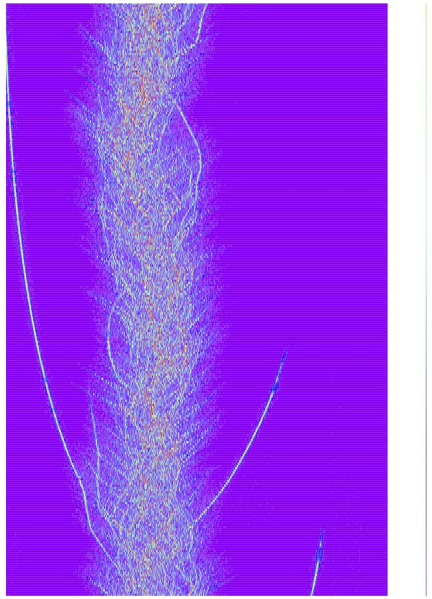

$Q_{sat} = 60$

Pulse propagation in SMF:

$$i\psi_z + \frac{D}{2}\psi_{tt} + |\psi|^2\psi = 0$$

Pulse propagation in EDF:

$$i\psi_z + \frac{D}{2}\psi_{tt} + G_2|\psi|^2\psi = \frac{ig_o}{1+Q/Q_{sat}}(\psi + b_2\psi_{tt})$$

Where the total energy is

$$Q = \int_{-\infty}^{\infty} |\psi|^2 dt$$

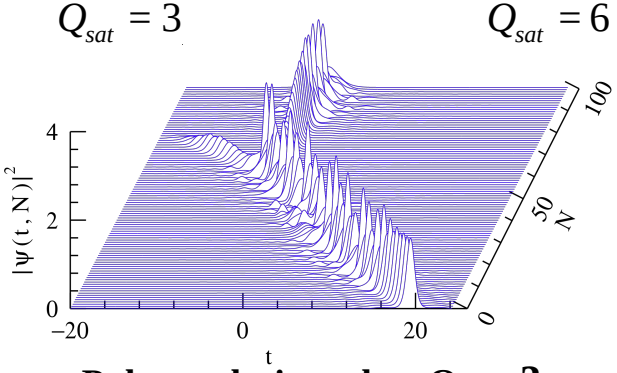

Pulse evolution when Q_{sat}= 3

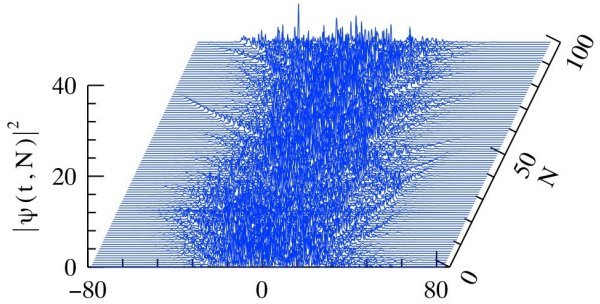

Pulse group evolution when Q_{sat}= 60

Dissipative solitons with energy and matter flows: fundamental building blocks for the world of living organisms

CGLE: $$i\psi_t + \frac{D}{2}\psi_{xx} + n(u,v)\psi + |\psi|^2\psi + n|\psi|^4\psi = i\delta\psi + i\beta\psi_{xx} + i\varepsilon|\psi|^2\psi + i\mu|\psi|^2\psi$$

RDS: $$\frac{\partial u}{\partial t} = -\nu - u(u-1)(u-a) + u_{xx}$$

$$\frac{\partial v}{\partial t} = \varepsilon_1(u - bv)$$

Coupling: $$a = a_0 + a_1|\psi|^2$$

$$n = n_0 + \Delta n(u - v)$$

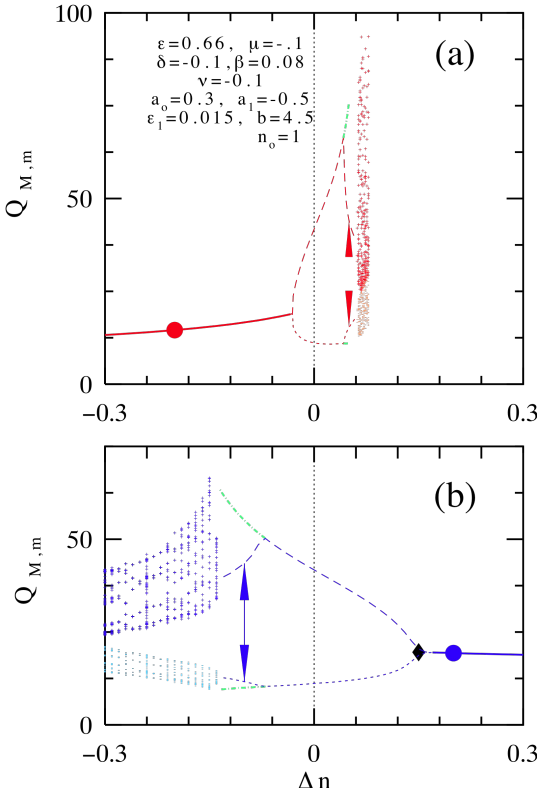

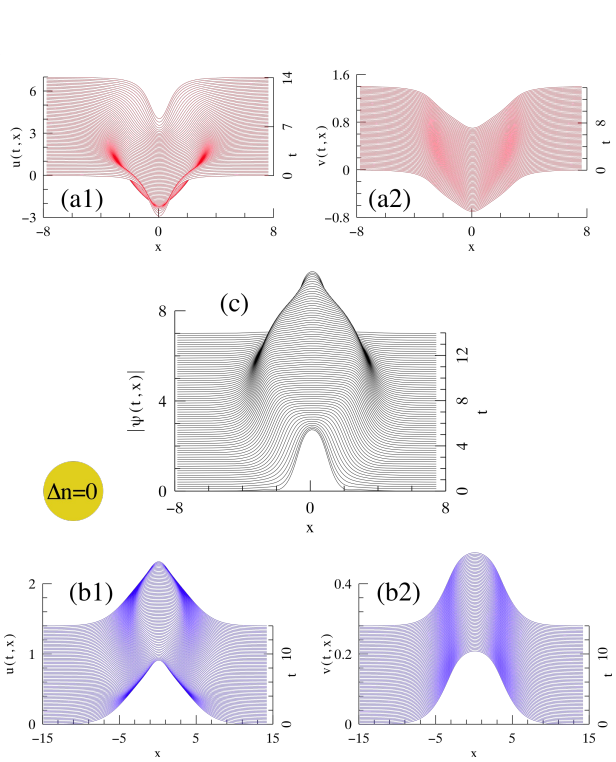

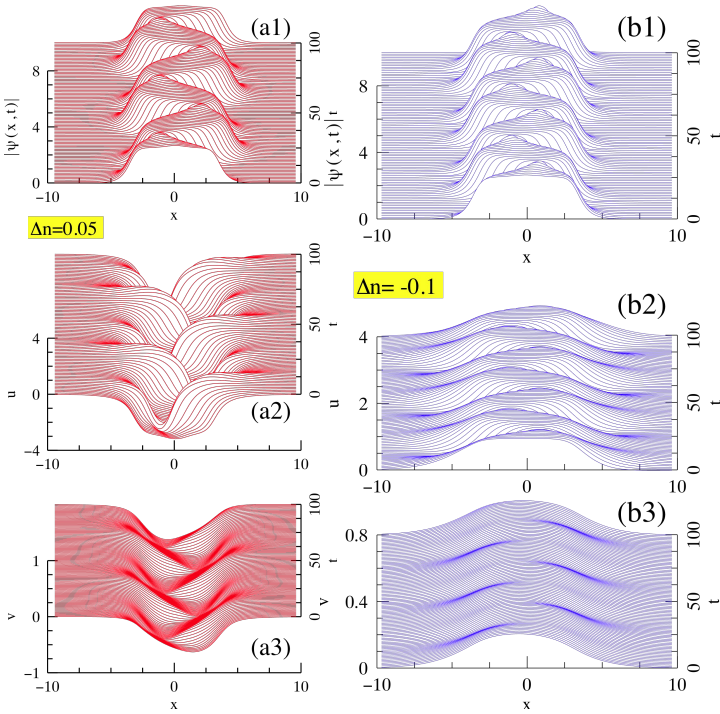

Energy rate equation:

$$\frac{\partial Q}{\partial t} = 2\int_{-\infty}^{\infty}[b|\psi_x|^2 + d|\psi|^2 + e|\psi|^4 + m|\psi|^6]dx$$

$$Q = \int_{-\infty}^{\infty}|\psi|^2 dx$$

The rate of change of total matter:

$$\frac{\partial M}{\partial t} = -e_1\int_{-\infty}^{\infty}[u_x^2 + bv^2 + u^2(u-1)(u-a)]dx$$

$$M = \int_{-\infty}^{\infty}(e_1u^2 + v^2)dx$$

H. R. Brand et al.

Dissipative rogue waves: numerical results

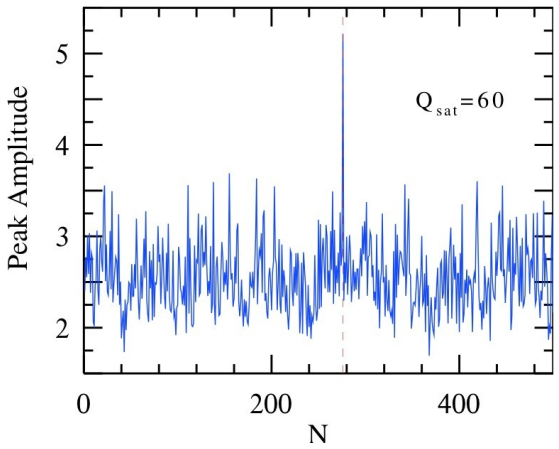

A sample of output radiation

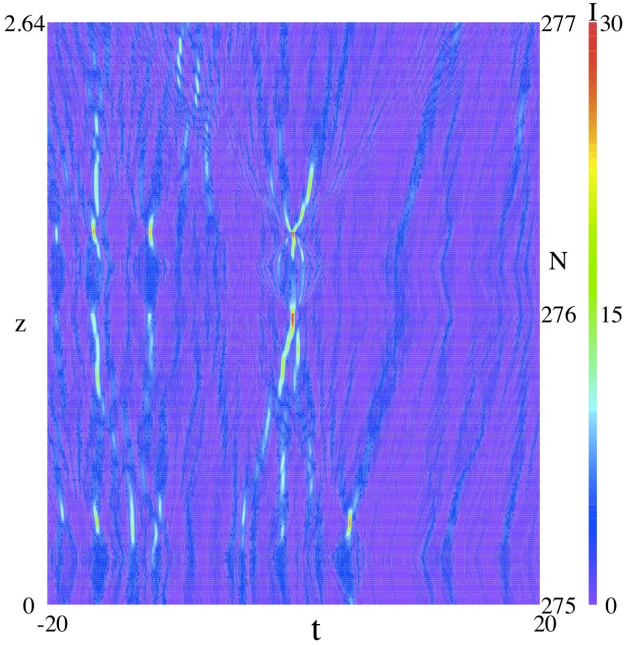

Two round trips containing the highest amplitude

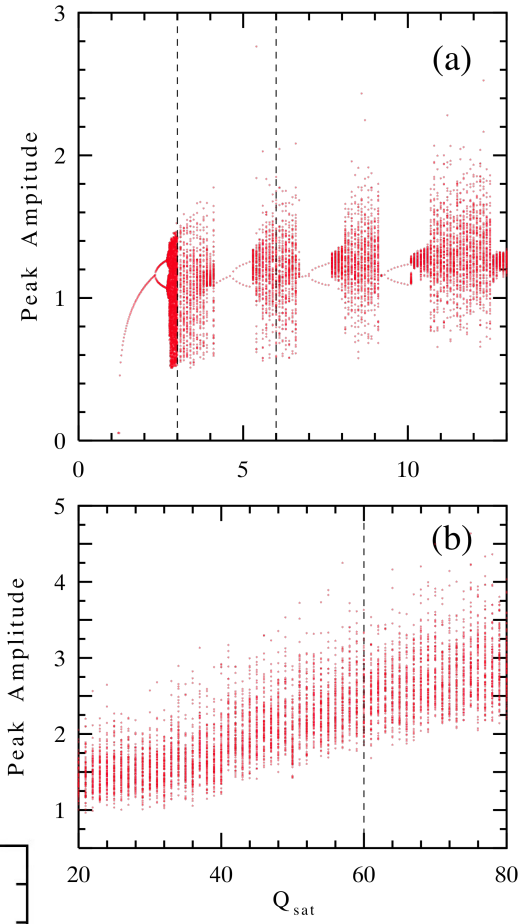

Bifurcation diagram

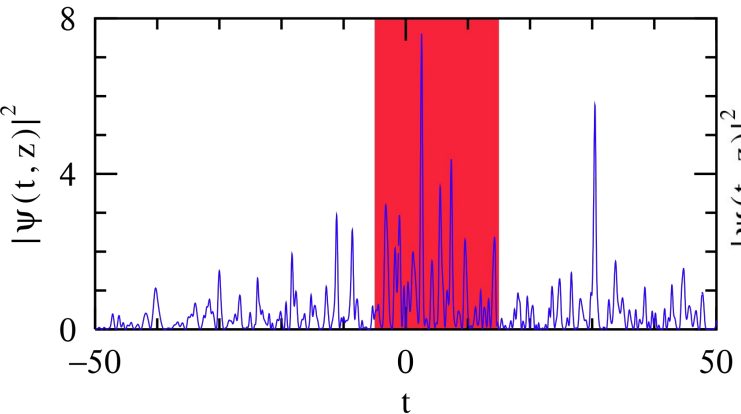

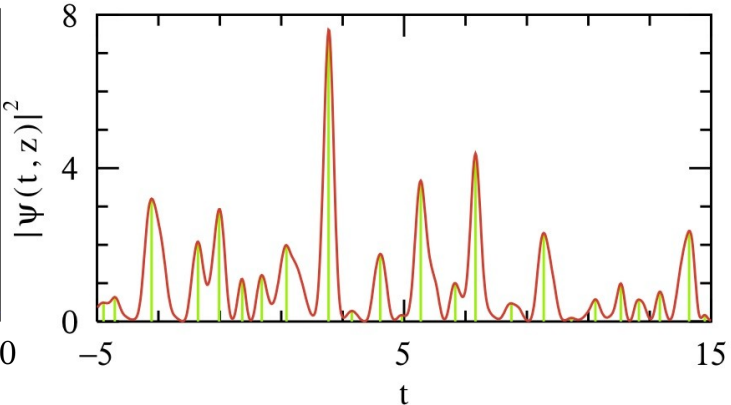

Dissipative solitons with energy and matter flows: internal balances

$$\frac{\partial \rho}{\partial t} + \frac{\partial j}{\partial x} = p$$

$$\rho = |\psi|^2$$

$$j = \frac{iD}{2}(\psi \psi_x^* - \psi \psi_x^*)$$

$$p = 2d|\psi|^2 + 2e|\psi|^4 + b(|\psi|^2)_{xx} - 2b|\psi_x|^2$$

$$\frac{\partial m}{\partial t} + \frac{\partial J}{\partial x} = P$$

$$m = e_1 u^2 + v^2$$

$$J = -2e_1 u_x u$$

$$P = -2e_1[u_x^2 + bv^2 + u^2(u-1)(u-a)]$$

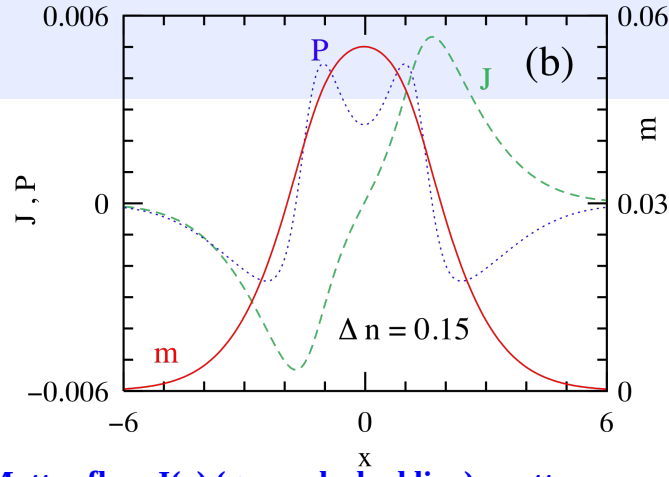

Matter flow J(x) (green dashed line), matter distribution m(x) (red curve) and density of matter generation P (x) (blue dotted curve) across the same stationary soliton.

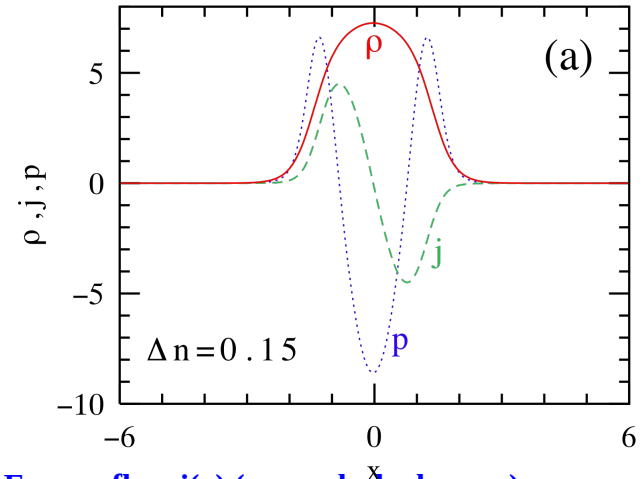

Energy flow j(x) (green dashed curve), energy distribution ρ(x) (red curve) and density of energy generation p(x) (blue dotted curve), across the stationary soliton at Δn = 0.15

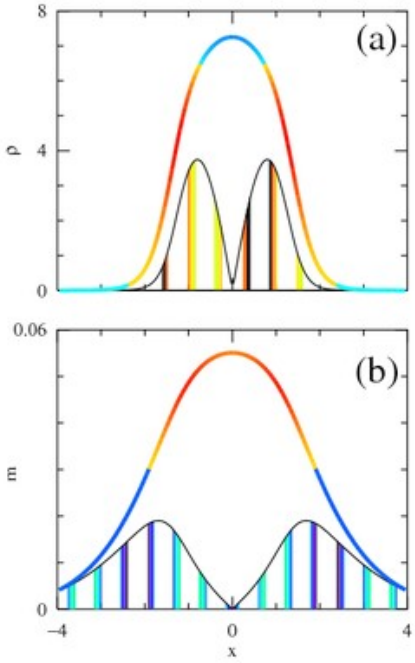

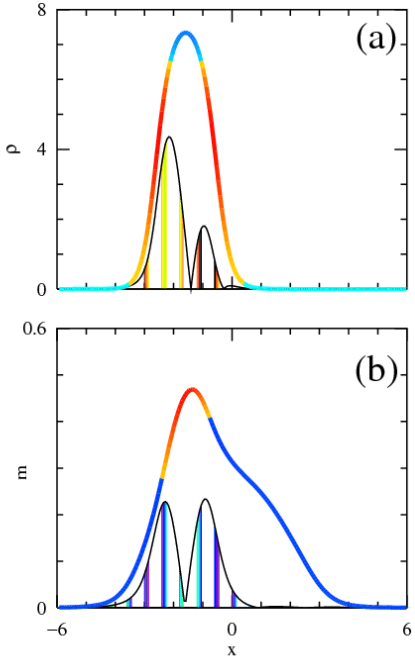

Dissipative rogue waves: Probability density functions

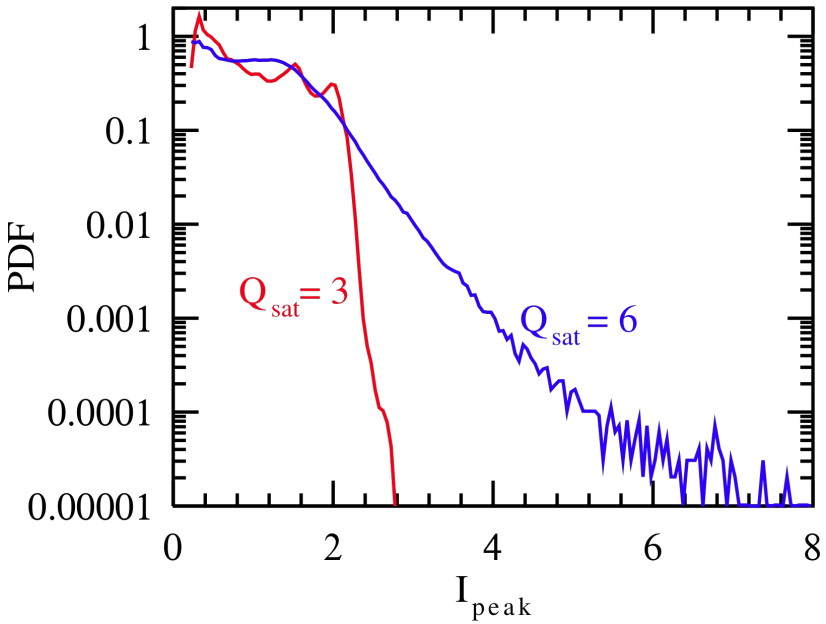

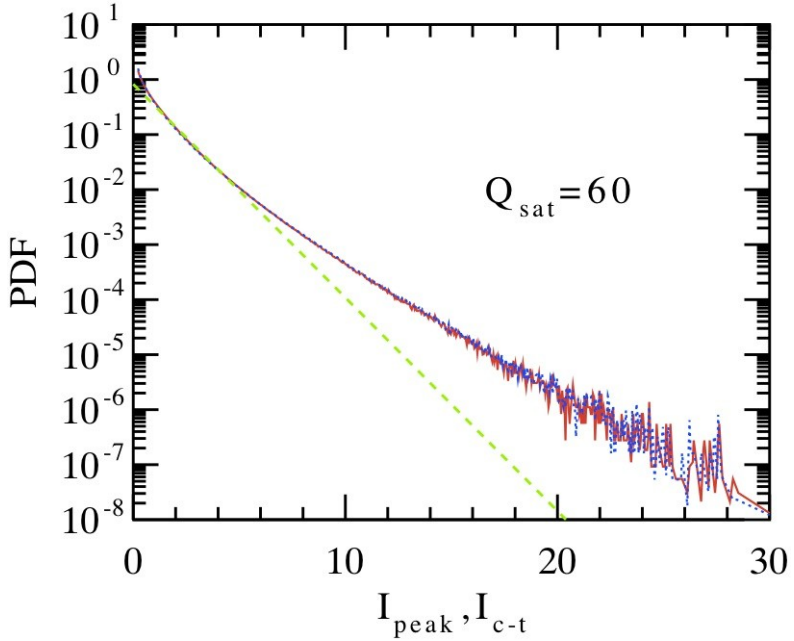

Probability density functions

Dissipative Rogue Waves, Experiment

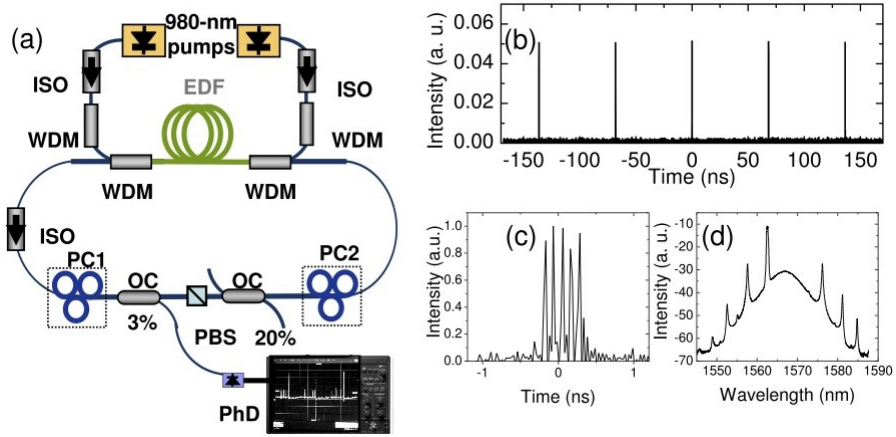

(Left) (a) Fiber laser experimental setup.

(b) Temporal trace of a stationary bunch of pulses circulating at the fundamental cavity repetition rate of 17.2 MHz.

(c) temporal magnification of the 1-ns-long bunch using a 20-GHz oscilloscope with a 45-GHz photodiode.

(d) Optical spectrum.

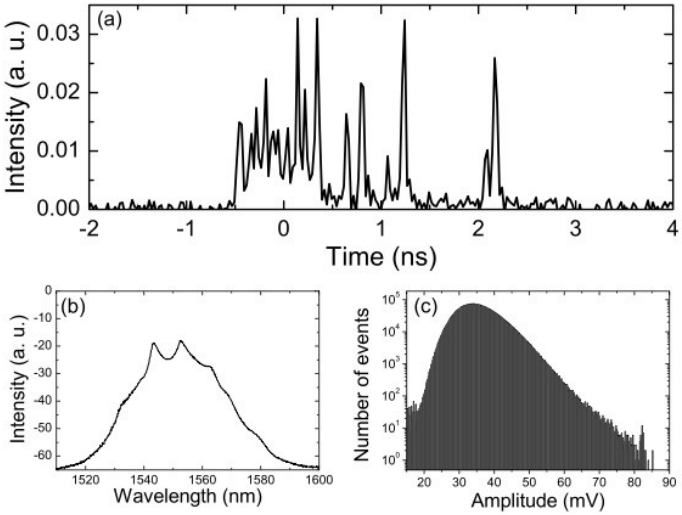

(a) Histogram (log-scale) showing a large deviation above the classical distribution (indicated by the yellow dotted-line) for 6.8 millions of trace events. RW events are observed at the level of up to 3 times the SWH.
(b) Optical spectrum.
(c) Optical autocorrelation trace, with a close-up view of the central coherence peak (inset).
(d) Stroboscopic recording showing the intracavity evolution over successive roundtrips around a rogue wave event.

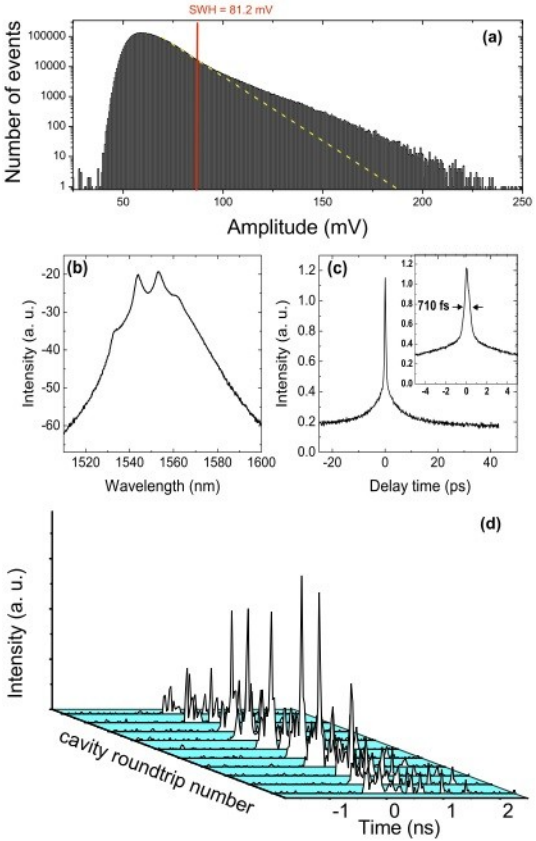

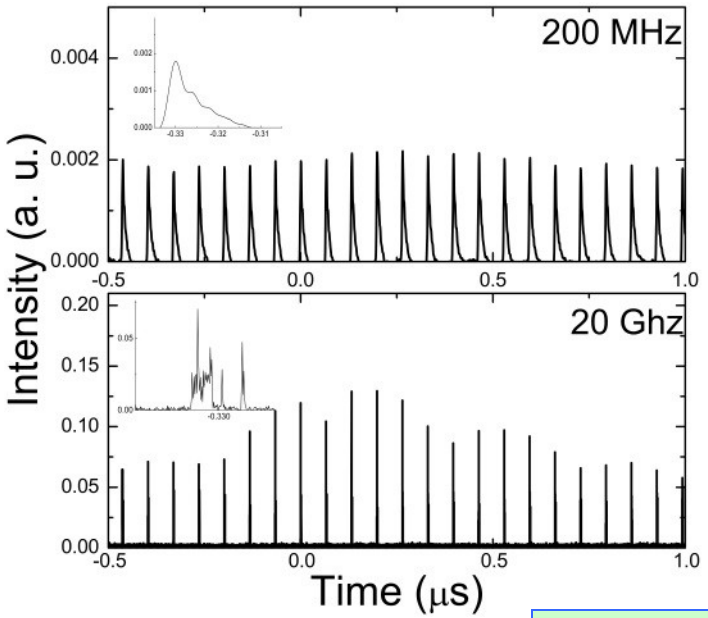

(Above) (a) Optical intensity record of a chaotic bunch of pulses (b) Optical spectrum (c) Histogram (log-scale) showing the distribution of the optical intensity maxima for 4.9 millions of trace events. SWH is 41.9 mV

(Left) Comparison between narrow (a) 200 MHz and wide (b) 20 GHz electronic bandwidth analysis of the same sequence of laser output pulse events. Insets: One pulse event is magnified in both cases.

PRL **108**, 233901 (2012)

FPU Recurrence and Cherenkov radiation

$$i\frac{\partial y}{\partial z}+\frac{b_2}{2}\frac{\partial^2 y}{\partial t^2}+|y|^2 y=ib_3\frac{\partial^3 y}{\partial t^3}$$

Dispersive waves:

$$\psi=\mu\exp(ikz-iwt)$$

The frequency satisfies the dispersion relation:

$$-k-\frac{w^2 b_2}{2}=-b_3 w^3$$

Continuous wave: $\psi=B\exp(iB^2 z)$

$$\psi(z,t)=\left[1-\frac{\frac{W^2}{2}\cosh(dz)+id\sinh(dz)}{\cosh(dz)-\frac{d}{W}\cos(Wt)}\right]e^{iz}$$

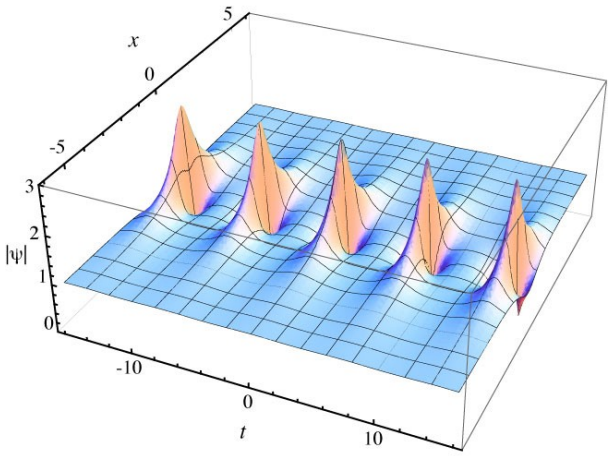

Resonant condition:

$$B^2=1=-\frac{w^2 b_2}{2}+b_3 w^3$$

Then we have the cubic equation to solve:

$$\omega^3-\frac{b_2}{2b_3}w^2-\frac{1}{b_3}=0$$

Growth rate: $\delta=\Omega\sqrt{1-\frac{W^2}{4}}$

Spectra:

$$A_0(z)=\left[1-\frac{\frac{W^2}{2}\cosh(dz)+id\sinh(dz)}{\sqrt{\cosh^2(dz)-\frac{d^2}{W^2}}}\right]$$

The real solution: $\omega=\frac{\chi^2+b_2 c+b_2^2}{6b_3 c}$

$$A_n(z)=\frac{\frac{W^2}{2}\cosh(dz)+id\sinh(dz)}{\sqrt{\cosh^2(dz)-\frac{d^2}{W^2}}}\left[\cosh(dz)-\sqrt{\cosh^2(dz)-\frac{d^2}{W^2}}\right]^{|n|}$$

where:

$$\chi=(\beta_2^3+108b_3^2+6\sqrt{6}\sqrt{b_2^3 b_3^2+54b_3^4})^{1/3}$$

FPU Recurrence and radiation

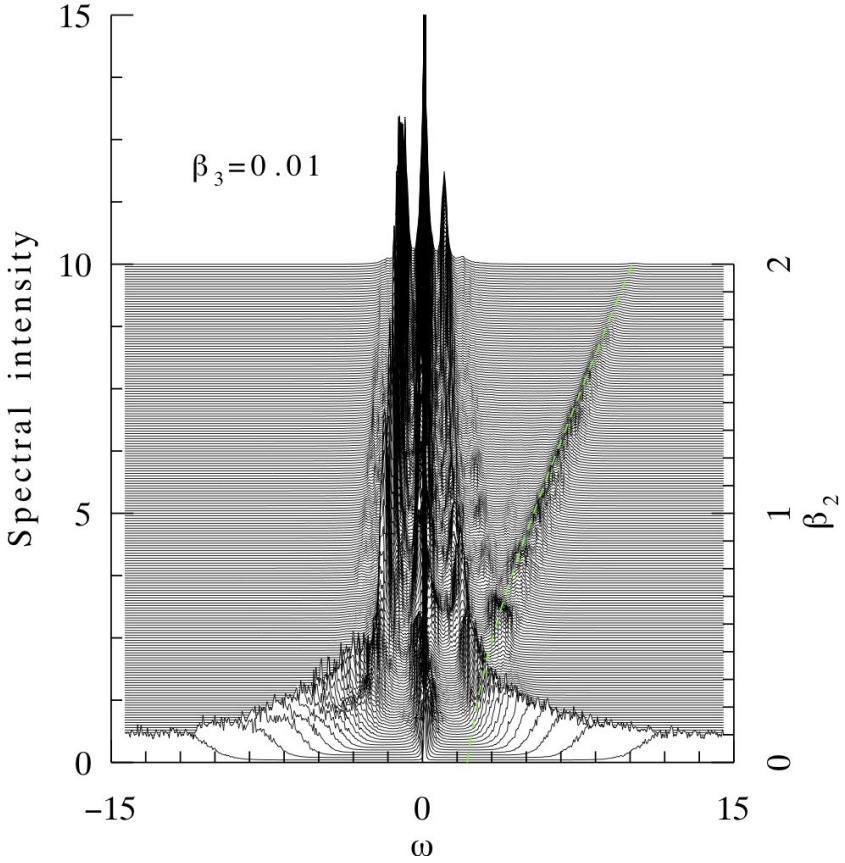

Spectral output for a propagation distance z=20, β3=0.01 and for various values of β2. The two sidebands are related to modulation instability, while the additional spectral band on the right represents the resonant radiation.

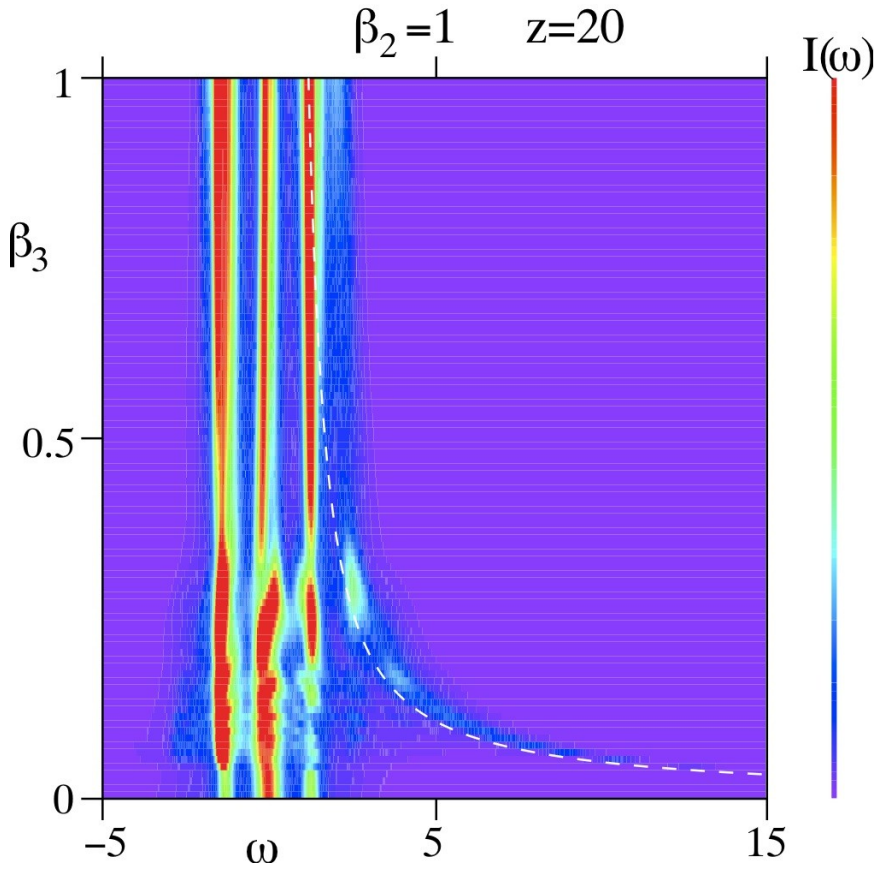

Spectral output for a propagation distance z=20, β2=1 as a function of β3

Soto-Crespo, Ankiewicz, Devine and Akhmediev, JOSA B 29, 1930 (2012)

FPU Recurrence and radiation

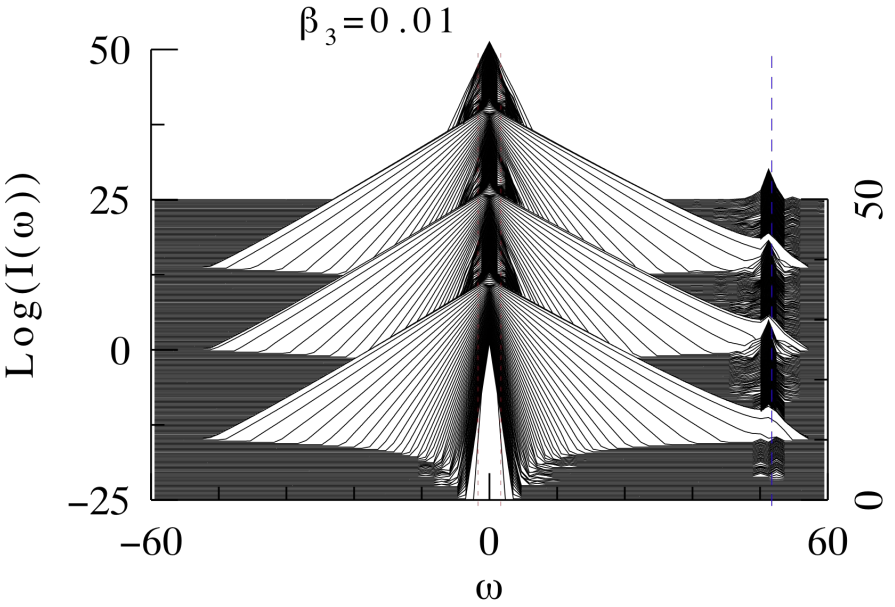

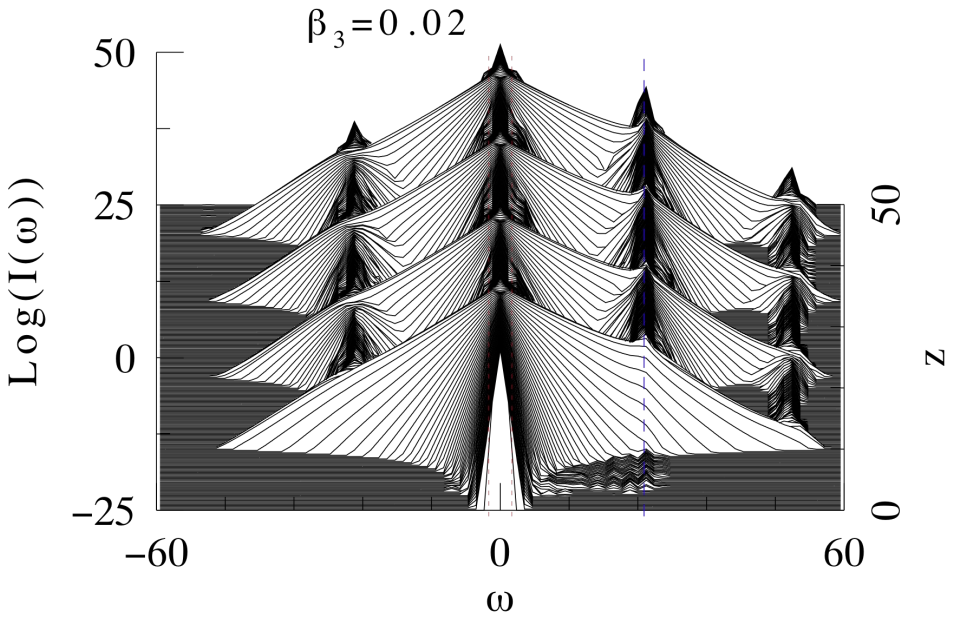

Recurrence spectrum of the NLSE with small TOD, β3=0.01, and β2=1. The resonant radiation that can be seen on the r.h.s. of the spectrum is indicated by the dashed blue line. Its influence is negligible until the radiation grows to higher amplitudes and distorts the initially symmetric AB spectrum. However, this distortion occurs at very long propagation distances. The two red vertical lines show the limits of the modulation instability region (±2). The initial condition contains only a single pair of sidebands at the maximum growth rate ω=sqrt(2). The periodicity is preserved on propagation by imposing periodic boundary conditions, such that the whole spectrum remains discrete.

The TOD is higher: β3=0.02. Resonant radiation is now closer to the pump. It hardly influences the first recurrence, but due to the FWM through the pump, the resonant radiation appears almost symmetrically on the left-hand-side of the spectrum. Moreover, an additional ``sideband'' of the resonant radiation appears at an equal distance on the right-hand-side of the spectrum. The asymmetry between the lhs. and rhs of the spectrum is due to the delay in the transfer of the spectral energy to the left-hand-side of the spectrum.

Soto-Crespo, Ankiewicz, Devine and Akhmediev, JOSA B 29, 1930 (2012)

FPU Recurrence and radiation

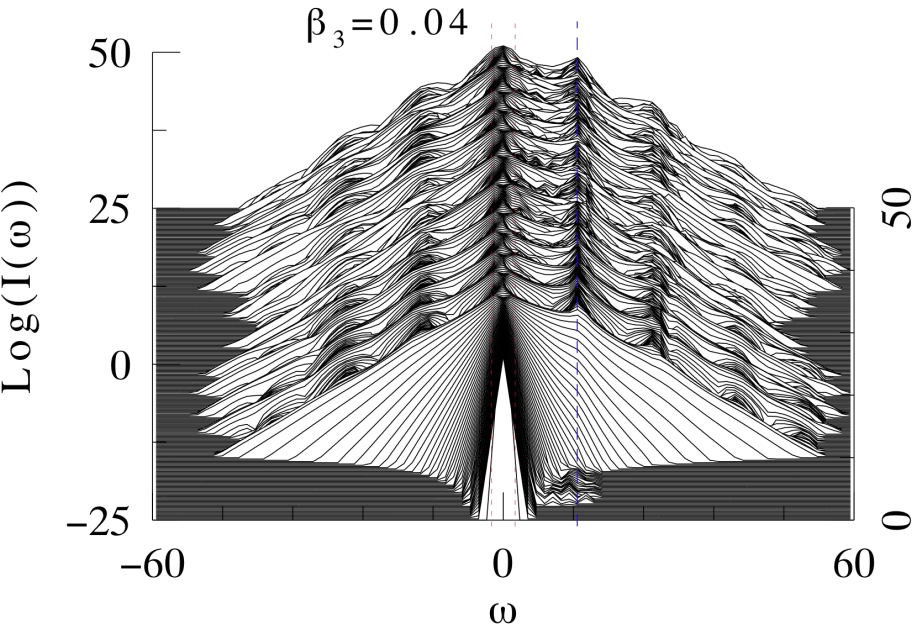

The TOD is further increased to β3=0.04. The resonant radiation (shown by the blue dashed line) is now much closer to the pump, but is still out of the instability band shown by the red dashed lines. The four-wave mixing adds distortions on each side of the spectrum. The resonant radiation appears at higher values of the background spectrum, thus increasing its influence. It accumulates much faster and FPU recurrence is lost right from the first broadening of the spectrum. No cycles of recurrence can be seen here.

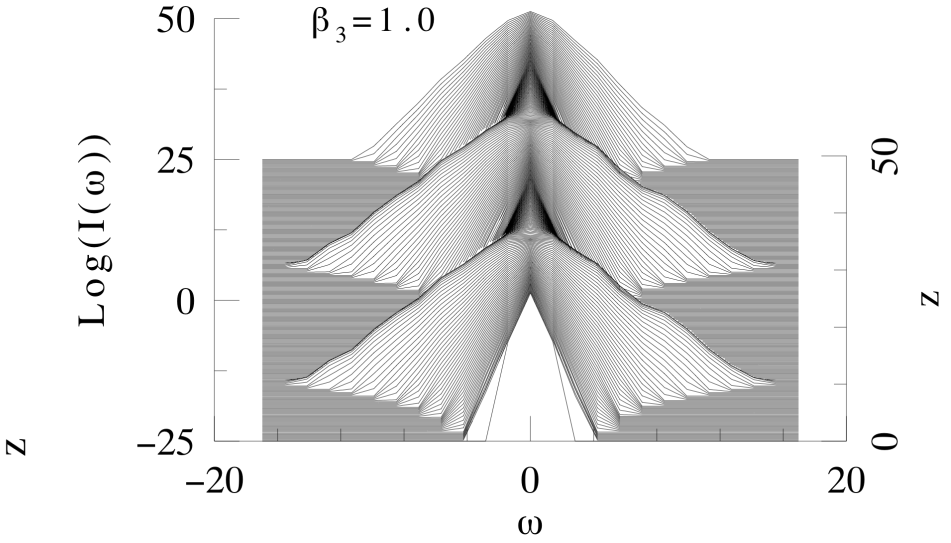

FPU recurrence dynamics of MI with almost perfect triangular spectrum of the sidebands when β3=1. The resonant frequency here is within the MI band. It defines the fundamental frequency of the sidebands.

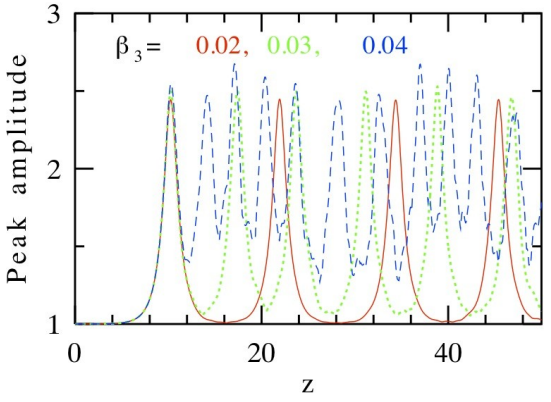

Field evolution, starting with modulation instability, for three small values of TOD. The solid red curve is for β3=0.02, the green dotted line is for β3=0.03, and the blue dashed curve for β3=0.04. Up to z=12, the three curves almost coincide. Multiple recurrence is clearly seen at the initial stages of evolution for the smallest values of β3. Increasing the TOD parameter causes the periodic behavior to deteriorate.

FPU Recurrence and radiation

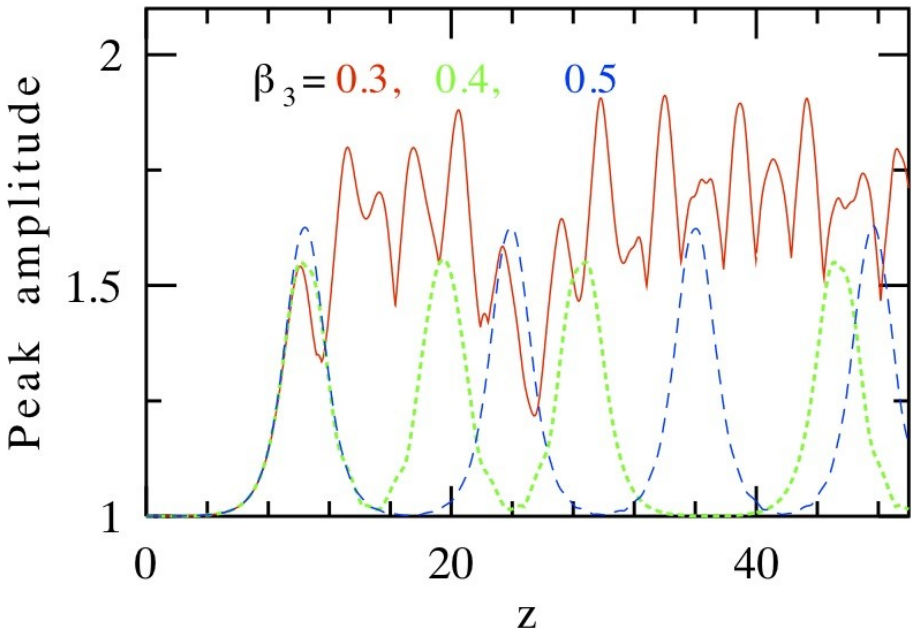

Optical field evolution, starting with modulation instability for three larger values of TOD: the red solid line stands for β3=0.3, the green dotted line for β3=0.4 and the dotted blue line for β3=0.5. Recurrence, which was lost for small values of β3, starts to be seen again for larger values of TOD, namely for β3> 0.3.

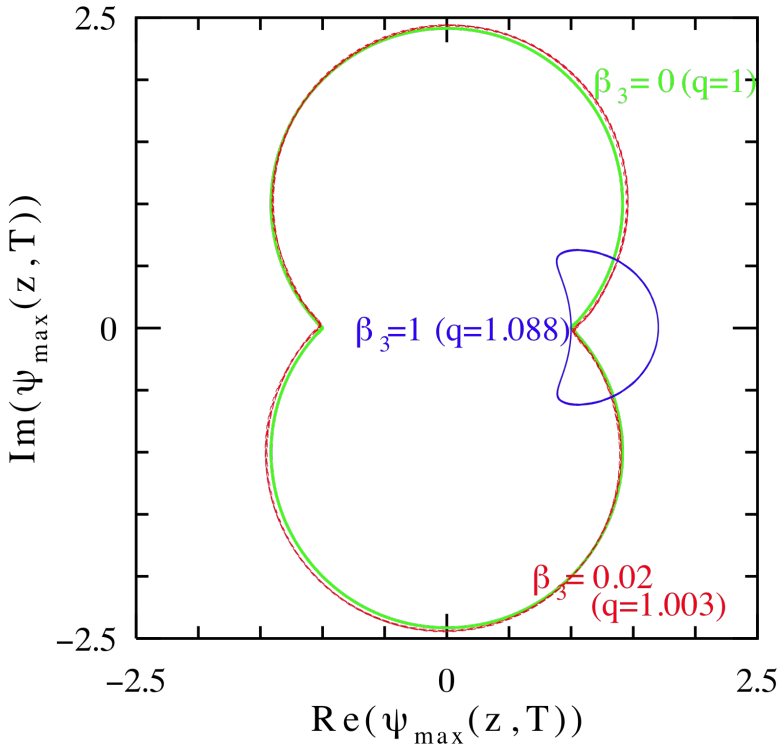

Recurrent trajectories of MI dynamics for β3=0 (green curve), β3=0.02 (red curve) and β3=1 (blue curve).

VOLUME 87, NUMBER 3 PHYSICAL REVIEW LETTERS 16 JULY 2001

Experimental Demonstration of the Fermi-Pasta-Ulam Recurrence in a Modulationally Unstable Optical Wave

G. Van Simaeys, Ph. Emplit, and M. Haelterman
Service d'Optique et d'Acoustique, Université Libre de Bruxelles, 50 Avenue F.D. Roosevelt, CP 194/5, B-1050 Brussels, Belgium
(Received 19 March 2001; published 28 June 2001)

The END